Rotation–vibration spectra of icosahedral molecules. II. Icosahedral symmetry, vibrational eigenfrequencies, and normal modes of buckminsterfullerene

David E. Weeks and William G. Harter
Los Alamos National Laboratory T-12, Los Alamos New Mexico 87545 and Department of Physics, J. William Fulbright College of Arts and Sciences, Unversity of Arkansas, Fayetteville Arkansas 72701

(Received 4 August 1988; accepted 14 December 1988)

The icosahedral symmetry of molecules such as buckyball, $B_{12}H_{12}^{-2}$, and $C_{20}H_{20}$, is analyzed using subgroup chain defined projection operators. The icosahedral analysis is used to determine the eigenvalues and eigenvectors of a classical spring mass model of buckyball. A spectrum of Raman and dipole active modes is given using the spring constants of benzene. Corresponding dipole active and Raman active normal modes are displayed stereographically. Several choices for springs constants are discussed and a comparison with spring mass systems of reduced symmetry is made.

I. INTRODUCTION

In his famous treatise on group theory, Hamermesch makes the statement that the "icosahedral group has no physical interest and no examples of molecules with this symmetry are known.[1]" Today we know that this is not the case and that there are at least two molecular structures with icosahedral symmetry. These are the better known borohydride anion $B_{12}H_{12}^{-2}$ (Ref. 2) and the recently synthesized dodecahedrane $C_{20}H_{20}$.[3] Both molecules have an icosahedrally symmetry framework that forms an empty cage with no central atom.[4] For $B_{12}H_{12}^{-2}$ the boron atoms are positioned at the vertices of an icosahedron as in Fig. 1(a), while in dodecahedrane the carbon atoms define a dodecahedral framework dual to the icosahedron as in Fig. 1(b). In each case the icosahedral structure of the molecule has been verified using x-ray diffraction.[5,6] The B–B separation (1.77 Å) and the C–C separation (1.5 Å) were measured and with these values the diameter of the inner cavities of $B_{12}H_{12}^{-2}$ and $C_{20}H_{20}$ are found to be 3.4 Å and 4.2 Å, respectively.

Several theoretical studies have considered the question of encapsulating small atoms or ions such as H, H^+, Li, Li^+, or He in the dodecahedral cavity of $C_{20}H_{20}$.[7–9] These chemically exciting prospects encourage the search for larger cage molecules. One possibility that dwarfs $B_{12}H_{12}^{-2}$ and $C_{20}H_{20}$ is the proposed icosahedrally symmetric buckminsterfullerene or buckyball structure of C_{60} shown in Fig. 1(a).[10] Theoretical calculations indicate an average buckyball C–C bond length of 1.4 Å (Ref. 11) and a cavity 7 Å in diameter. At present there is already experimental evidence for the encapsulation of single Ca, Ba, Sr, and La atoms.[12]

In order to better understand the encapsulation properties of C_{60} as well as other interesting behaviors, the determination of its specific structure is imperative. At present no known samples of C_{60} in crystalline from exist thereby ruling out x-ray diffraction. However, there remains the analysis and assignment of structurally dependent spectra. In previous works[13,14] we have calculated the rotational fine and superfine spectral patterns expected for all molecules with icosahedral symmetry. Experimental observation of these patterns would verify the icosahedral structure of C_{60}. However, since extremely high resolution is required to observe the rotational superfine pattern, an easier experiment would be the observation of the infrared vibrational spectrum of C_{60}. The main purpose of this paper is to present a set of synthetic vibrational eigenvalue trajectories of buckyball to be used in the assignment of such an experimental infrared spectrum.[15] The general computational procedure involves icosahedral symmetry projection methods coupled with numerical diagonalization of matrices of eight dimensions or less. Several test cases are examined and found to agree with independent analytic results. In addition to eigenvalue trajectories we also present three-dimensional stereo figures of corresponding symmetry labeled normal modes. Proper symmetry labeling of normal modes is very useful in the calculation of perturbations such as rotational coriolis effects and isotope effects. Because our procedure involves the diagonalization of at most an eight-dimensonal matrix it is possible to calculate eigensolutions and make stereo animated movies of the corresponding normal modes in just a few seconds on a MacIntosh 512K personal computer.

Previously and independently, vibrational eigenvalues of buckyball have been reported by Wu, Jelski, and George.[16] Their computational procedure involved the direct diagonalization of a 180-dimensional matrix. The reported results included values for the same test cases for which analytic results are available. Serious discrepancies between the numerical results of Ref. 16 and the analytic eigenvalues for the test cases invalidate their prediction for buckyball eigenfrequencies. The derivation and comparison of the analytic results with the test cases is given in Appendix A. Using modified neglect of diatomic overlap (MNDO) structure calculations and subsequent diagonalization of a 180-dimensional Cartesian force constant matrix, Stanton and Newton have also calculated a vibrational spectrum of buckyball.[17] Their results do not include calculation of the test cases, so analytic verification of their calculations has not been examined so far. However, differences between our results and theirs are probably due to the use of different force field models.

In addition to icosahedrally symmetric structures on the molecular level, there is a more pervasive existence of icosa-

 0021-9606/89/094744-28$02.10

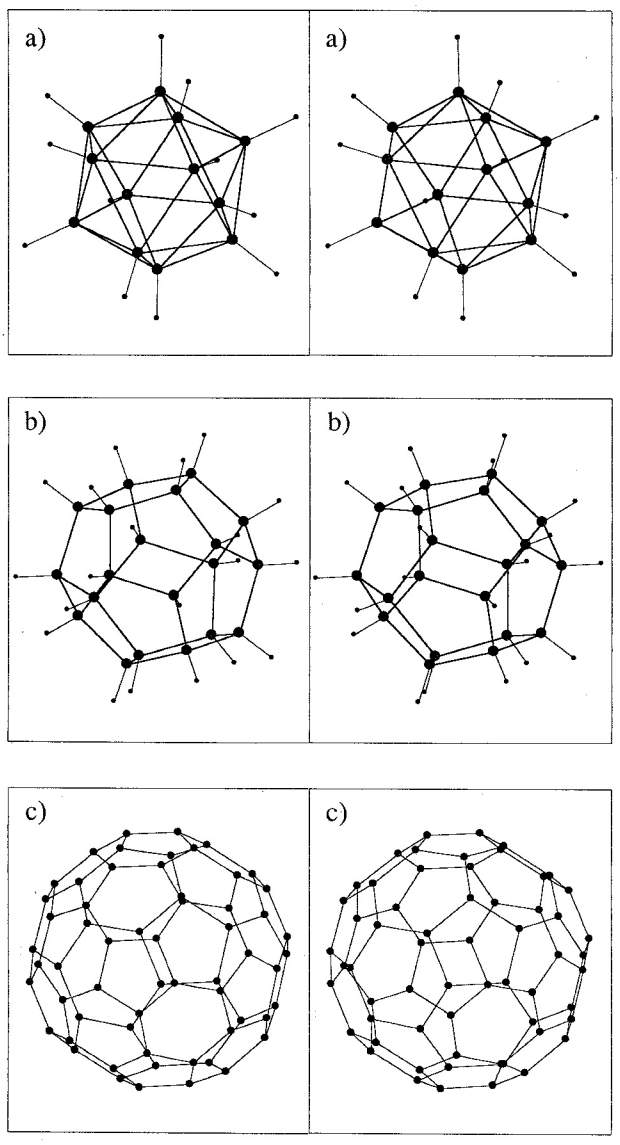

FIG. 1. Stereoscopic views of (a) the borohydride anion, $B_{12}H_{12}^{-2}$, (b) dodecahedrane, $C_{20}H_{20}$, and (c) buckyball, C_{60}.

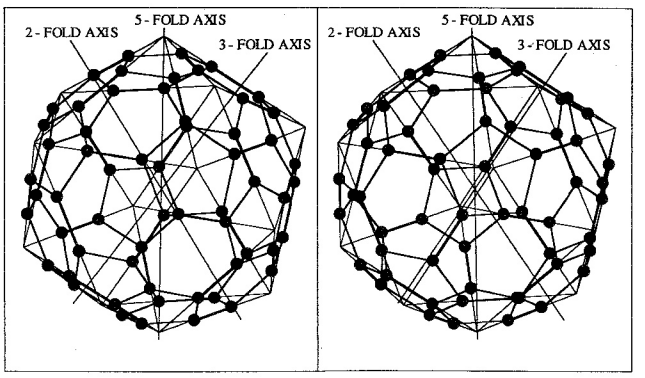

FIG. 2. Stereoscopic view of buckyball. "Double bonds" lie along the thick lines and "single bonds" lie along the thin lines. Carbon atoms are located at the vertices. An icosahedron is superimposed on the figure of buckyball to illustrate its icosahedral symmetry. Generic two, three, and fivefold symmetry axes are drawn and labeled.

hedral symmetry in the capsids of many virons. These include the rinoviruses involved in the common cold as well as more dangerous viruses that are causative agents in diseases such as polio, rubella and possibly even AIDS.[18–20]

II. ICOSAHEDRAL SYMMETRY

The full symmetry of buckyball is that of the icosahedral point group I_h which is the largest finite symmetry point group allowed in three-dimensional Euclidean space. By taking advantage of this symmetry it is possible to greatly reduce the amount of work needed to calculate rovibronic eigenvalues and eigenvectors. In addition, symmetry analysis neatly classifies these eigenvalues and provides a method for organizing the degenerate eigenvectors. This permits the selection of an optimal choice of basis when considering perturbations.

The 12 pentagonal and 20 hexagonal faces of buckyball correspond to the 12 vertices and 20 faces of the icosahedron. Smalley and co-workers have proposed that one carbon atom is located at each of the 60 vertices of this truncated icosahedron.[10] Each vertex lies in a symmetry plane of reflection but not along a symmetry axis of rotation. Thus, if any one of the 60 carbon atoms is isotopically different from the others the symmetry will be broken from I_h to simple bilateral reflection C_v. Carbon bonds are formed along the three edges that meet at each vertex. They are resonant bonds, and presumably those along the pentagonal edges are more like a single bond and those along an edge bordered by two hexagons are more like a double bond as illustrated in Fig. 2. In this fashion all valencies are satisfied while forming a highly aromatic and relatively stable spheroidal shell.[21]

The 120-element icosahedral point group of buckyball is the cross product of the 60-element icosahedral rotation group I and the inversion group C_I. The inversion group contains only the unit operator and inversion operator, both of which commute with the 60 rotations in group I. Each of the lab-fixed icosahedral rotation operators rotates an icosahedron *clockwise* by an angle ω about a twofold, threefold, or fivefold symmetry axis. This rotation angle ω divides the icosahedral rotations into five classes. These clasess are labeled C_1, C_R, C_{R^2}, C_r, and C_i and contain, 1, 12, 12, 20, and 15 operators, respectively. The class C_1 contains only the unit operator with a rotation angle $\omega_1 = 0°$. The classes C_R and C_{R^2} contain all rotations about fivefold symmetry axes with rotation angles $\omega_R = 72°$ and $\omega_{R^2} = 144°$. The class C_r contains all threefold symmetric rotations with $\omega_r = 120°$, and the class C_i contains all twofold symmetry rotations with $\omega_i = 180°$. All group operators in each class, and their symmetry axes, are shown in Fig. 3.

The elements of the full icosahedral group I_h are generated by first operating on all the rotations of I with the unit operator of C_I, replicating the class structure of the group I. Then, all the rotations of the group I are multiplied with the inversion operator of C_I, creating 60 new improper rotations and five new classes. This yields a total of 120 operators and 10 classes in the full icosahedral group I_h. Group operators and class structure of I_h are given in Fig. 4, and an icosahedral group multiplication table for rotations only is given in

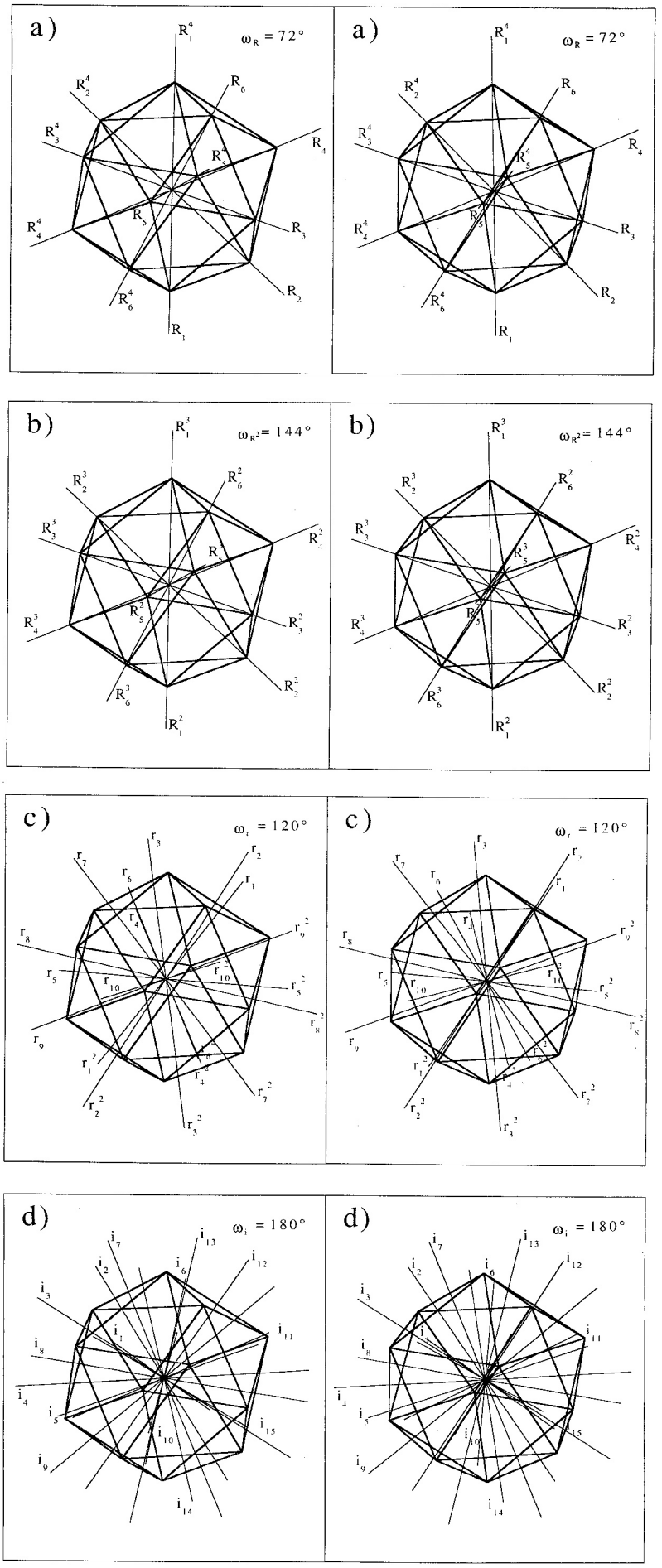

FIG. 3. Icosahedral rotation operators and symmetry axes of the classes (a) C_R, (b) C_{R^2}, (c) C_r, and (d) C_i.

Icosahedral {I} Class Structure				Icosahedral $\{I_h\}$ Class Structure			
$C_1 = 1$				$C_I = I$			
C_R	C_{R^2}	C_r	C_i	C_ρ	C_{ρ^2}	C_η	C_σ
$\omega=72$	$\omega=144$	$\omega=120$	$\omega=180$				
R_1	R_1^2	r_1	i_1	$I\ R_1=\rho_1$	$I\ R_1^2=\rho_1^2$	$I\ r_1=\eta_1$	$I\ i_1=\sigma_1$
R_2	R_2^2	r_2	i_2	$I\ R_2=\rho_2$	$I\ R_2^2=\rho_2^2$	$I\ r_2=\eta_2$	$I\ i_2=\sigma_2$
R_3	R_3^2	r_3	i_3	$I\ R_3=\rho_3$	$I\ R_3^2=\rho_3^2$	$I\ r_3=\eta_3$	$I\ i_3=\sigma_3$
R_4	R_4^2	r_4	i_4	$I\ R_4=\rho_4$	$I\ R_4^2=\rho_4^2$	$I\ r_4=\eta_4$	$I\ i_4=\sigma_4$
R_5	R_5^2	r_5	i_5	$I\ R_5=\rho_5$	$I\ R_5^2=\rho_5^2$	$I\ r_5=\eta_5$	$I\ i_5=\sigma_5$
R_6	R_6^2	r_6	i_6	$I\ R_6=\rho_6$	$I\ R_6^2=\rho_6^2$	$I\ r_6=\eta_6$	$I\ i_6=\sigma_6$
R_1^4	R_1^3	r_7	i_7	$I\ R_1^4=\rho_1^4$	$I\ R_1^3=\rho_1^3$	$I\ r_7=\eta_7$	$I\ i_7=\sigma_7$
R_2^4	R_2^3	r_8	i_8	$I\ R_2^4=\rho_2^4$	$I\ R_2^3=\rho_2^3$	$I\ r_8=\eta_8$	$I\ i_8=\sigma_8$
R_3^4	R_3^3	r_9	i_9	$I\ R_3^4=\rho_3^4$	$I\ R_3^3=\rho_3^3$	$I\ r_9=\eta_9$	$I\ i_9=\sigma_9$
R_4^4	R_4^3	r_{10}	i_{10}	$I\ R_4^4=\rho_4^4$	$I\ R_4^3=\rho_4^3$	$I\ r_{10}=\eta_{10}$	$I\ i_{10}=\sigma_{10}$
R_5^4	R_5^3	r_1^2	i_{11}	$I\ R_5^4=\rho_5^4$	$I\ R_5^3=\rho_5^3$	$I\ r_1^2=\eta_1^2$	$I\ i_{11}=\sigma_{11}$
R_6^4	R_6^3	r_2^2	i_{12}	$I\ R_6^4=\rho_6^4$	$I\ R_6^3=\rho_6^3$	$I\ r_2^2=\eta_2^2$	$I\ i_{12}=\sigma_{12}$
		r_3^2	i_{13}	I_h Class Operators		$I\ r_3^2=\eta_3^2$	$I\ i_{13}=\sigma_{13}$
		r_4^2	i_{14}	$cR=\sum_{n=1}^{6} R_n+R_n^4$	$c\rho=I\ cR$	$I\ r_4^2=\eta_4^2$	$I\ i_{14}=\sigma_{14}$
		r_5^2	i_{15}			$I\ r_5^2=\eta_5^2$	$I\ i_{15}=\sigma_{15}$
		r_6^2		$cR^2=\sum_{n=1}^{6} R_n^2+R_n^3$	$c\rho^2=I\ cR^2$	$I\ r_6^2=\eta_6^2$	
		r_7^2				$I\ r_7^2=\eta_7^2$	
		r_8^2		$cr=\sum_{n=1}^{10} r_n+r_n^2$	$c\eta=I\ cr$	$I\ r_8^2=\eta_8^2$	
		r_9^2				$I\ r_9^2=\eta_9^2$	
		r_{10}^2		$ci=\sum_{n=1}^{15} i_n$	$c\sigma=I\ ci$	$I\ r_{10}^2=\eta_{10}^2$	

FIG. 4. Class structure of the full icosahedral group I_h. The relation between proper and improper rotations of I_h is given in the four right-hand columns. Class structure of the icosahedral rotation group I is shown in the highlighted box and corresponds to the rotational in Fig. 3. Class operators are sums over corresponding class elements.

Fig. 5. Products of the improper rotations of I_h may be evaluated by first expressing the operators in terms of icosahedral rotations and inversion using Fig. 4. Then, by using the commutivity of the inversion operator and icosahedral rotations, the resulting product of rotations may be evaluated using Fig. 5. For example,

$$\rho_3^2\sigma_4 = I R_3^2 I i_4 = I I R_3^2 i_4 = R_6^4 ,$$

where the inversion group product $II = 1$ was used. Characters and irreducible representations of the icosahedral group are given in Appendix B.

III. THE FORCE CONSTANT MATRIX

The vibrational eigenvalues and normal modes of buckyball are calculated by applying Newton's 2nd law to a classical spring-mass model. Icosahedral symmetry analysis is used to diagonalize the resulting force constant matrix. In the model, carbon bonds are treated in the harmonic limit as springs that obey Hookes' law, and carbon nuclei are treated as point masses. The position of each mass is determined by one of 60 symmetrically placed orthogonal coordinate triads whose origins are located at the vertices of the buckyball structure. This symmetrically defined coordinate system is

1	R_1	R_2	R_3	R_4	R_5	R_6	R_1^4	R_2^4	R_3^4	R_4^4	R_5^4	R_6^4	R_1^2	R_2^2	R_3^2	R_4^2	R_5^2	R_6^2	R_1^3	R_2^3	R_3^3	R_4^3	R_5^3	R_6^3	r_1	r_2	r_3	r_4	r_5
R_1	R_1^2	r_7^2	r_6^2	R_3	r_1^2	R_5	1	R_4^2	R_6^4	r_2^2	R_2	r_3^2	R_1^3	i_3	i_1	r_9^2	i_{11}	r_4	R_1^4	r_8	r_{10}	i_9	r_5^2	i_{14}	R_4	R_6	R_2^4	r_5	R_3^4
R_2	r_3^2	R_2^2	r_7^2	r_8^2	R_1	R_3	R_4	1	R_5^4	R_6^4	r_5^2	r_4^2	i_{13}	R_3^2	i_2	i_4	r_1^2	r_{10}^2	r_2	R_2^4	r_6	r_9	i_{11}	i_{10}	R_4^2	r_9^2	R_6	R_5	R_4^4
R_3	r_7^2	r_8^2	R_3^2	r_9^2	r_6^2	r_{10}^2	R_6	R_5	1	R_1	R_4	R_2	i_7	i_8	R_3^3	i_9	i_6	i_{10}	r_3	r_5	R_3^4	r_2^2	r_1	r_4^2	r_2	R_6^2	r_4	R_5^2	r_1^2
R_4	R_2	r_5^2	r_8^2	R_4^2	R_3	r_9^2	r_2	R_6	R_1^4	1	r_1	R_5^4	r_3^2	i_{15}	i_3	R_4^3	r_6^2	i_5	i_{13}	r_4	r_7	R_4^4	i_6	r_{10}	i_{12}	i_9	R_6^2	r_{10}^2	R_5	
R_5	r_6^2	R_3	r_{10}^2	R_6	R_5^2	r_4	R_2^4	r_5	R_4^4	r_1^2	1	R_1	i_2	r_8^2	i_5	r_2	R_5^3	i_{14}	r_7	i_8	r_9	i_{12}	R_5^4	r_3^2	R_1^4	r_3	R_2^3	i_{15}	i_{11}	
R_6	R_3	R_4	r_9^2	r_2	r_{10}^2	R_6^2	r_3	r_4	R_2^4	R_5	R_1^4	1	r_7^2	r_5^2	i_4	i_{12}	i_1	R_6^3	i_7	i_{15}	r_8	r_1^2	r_6	R_6^4	R_1^3	i_{13}	i_{14}	i_{10}	R_5^2	
R_1^4	1	R_5^4	R_4	r_1	R_6	r_2	R_3^3	r_3	r_7	R_2^4	r_6	R_4^3	R_1	r_4^2	r_8^2	i_{11}	r_{10}^2	i_9	R_1^2	i_{14}	i_3	r_5	i_1	r_9	i_6	i_{12}	i_{13}	R_6^2	r_4	
R_2^4	R_5	1	R_6	R_1^4	r_4	r_3	r_7	R_2^3	r_8	r_5	R_3^4	R_4^4	r_6^2	R_2	r_9^2	r_1	i_{10}	i_{13}	i_2	R_2^2	i_4	i_{11}	r_{10}	r_2^2	r_6	R_3^3	i_7	i_{14}	i_{15}	
R_3^4	R_4^4	R_6^4	1	R_5^4	R_2^4	R_1^4	r_6	r_7	R_3^3	r_8	r_{10}	r_9	r_1^2	r_3^2	R_3	r_5^2	r_4	r_2	i_6	i_7	R_3^2	i_8	i_{10}	i_9	R_5^3	r_1	R_1^3	r_3	R_2^3	
R_4^4	r_7^2	R_1	R_5	1	r_5	R_2^4	R_3^4	r_8	r_9	R_5^4	R_6^4	r_2^2	i_6	r_7^2	r_{10}^2	R_4	i_{15}	r_3	r_6	i_3	i_5	R_4^2	r_4^2	i_{13}	R_4^5	R_1^4	r_7	R_2^3	i_8	
R_5^4	R_6^4	r_4^2	R_2	r_5^2	1	R_4	r_1	R_1^4	r_6	R_3^4	R_5^3	r_{10}	r_2^2	i_{14}	r_7^2	i_8	R_5	r_9^2	i_{12}	r_3	i_2	r_8	R_5^2	i_5	i_{11}	R_4^2	r_2	R_6	R_2^4	
R_6^4	r_2^2	r_3^2	R_1	R_2	R_4^4	1	R_5^4	R_3^4	r_{10}	r_9	r_4^2	R_6^3	i_{12}	i_7	r_6^2	r_8^2	r_5	R_6	r_1	r_7	i_1	i_4	i_{15}	R_6^2	r_5^2	R_4	R_1^4	R_2^4	r_8	
R_1^2	R_1^3	i_2	i_6	r_6^2	i_{12}	r_1^2	R_1	r_2^2	r_3^2	i_{13}	r_7^2	i_7	R_1^4	R_3^3	R_5^3	r_{10}^2	R_4^2	r_5	1	r_9	r_4^2	R_6^2	r_8^2	R_2^3	R_3	R_5	R_4^4	R_3^4	i_9
R_2^2	i_{14}	R_2^3	i_7	i_3	r_3^2	r_7^2	r_8^2	R_2	r_5^2	r_4^2	i_8	i_{15}	R_6^2	R_2^4	R_3^3	r_2^2	r_6^2	r_9^2	1	r_1	r_{10}	R_4^3	R_5^2	i_4	R_5^2	R_3	R_1	R_6^4	
R_3^2	i_3	i_4	R_3^3	i_5	i_2	i_1	r_{10}^2	r_6^2	R_3	r_7^2	r_9^2	r_8^2	R_3^2	R_3^4	R_4^4	R_6^3	R_1^3	R_5^3	r_4	r_1^2	1	r_3^2	r_2	r_5^2	R_6^2	i_{10}	R_5^2	i_6	R_1^2
R_4^2	r_5^2	i_{11}	i_8	R_4^3	r_8^2	i_4	i_9	r_9^2	r_2	R_4	i_{12}	r_1	r_4^2	R_5^2	R_2^3	R_4^4	r_7^2	R_3^3	R_6^3	r_{10}^2	r_3	1	R_1^2	r_6	r_2^2	r_9	i_5	R_3^2	R_3
R_5^2	i_1	r_{10}^2	i_{10}	r_4	R_5^3	i_{15}	r_5	i_{11}	r_1^2	i_6	R_5	r_8^2	R_3^3	r_9^2	R_6^3	r_3	R_4^5	R_2^2	r_8	R_4^2	r_2^2	R_1^3	1	r_7^2	R_4^2	R_3^2	i_8	r_5^2	r_1
R_6^2	r_9^2	r_2	i_9	i_{13}	i_5	R_6^3	i_{14}	i_{10}	r_4	r_{10}^2	r_3	R_6	r_8^2	r_1	R_4^3	R_1^2	R_3^3	R_4^6	R_2^2	R_5^3	r_5	r_6^2	r_7	1	i_7	r_3^2	r_4^2	r_{10}	i_1
R_1^3	R_1^4	r_6	r_1	i_6	r_2	i_{12}	R_1^2	i_{13}	i_7	r_3	i_2	r_7	1	r_{10}	r_5^2	R_5^2	r_9^2	R_3^4	R_1	R_6^3	R_2^2	r_4	R_3^2	r_8	r_6^2	r_1^2	r_2^2	i_9	R_6^2
R_2^3	r_4	R_2^4	r_3	r_7	i_{14}	i_7	i_3	R_2^2	i_8	i_{15}	r_8	r_5	r_{10}^2	1	r_2	r_6	R_6^3	R_1^2	R_5^2	R_2	R_4^2	R_5^3	r_9	r_1^2	R_3^3	i_2	r_7^2	r_3^2	r_4^2
R_3^3	r_8	r_9	R_4^3	r_{10}	r_7	r_6	i_1	i_2	R_5^3	i_3	i_5	i_4	r_5	r_2^2	1	r_4^2	r_3	r_1	R_5^2	R_1^2	R_3	R_2^2	R_6^2	R_4^3	i_{10}	R_5^3	i_6	R_1^3	i_7
R_4^3	i_{11}	r_1^2	r_5	R_4^4	i_8	r_8	r_9	i_4	i_9	R_4^2	r_2^2	i_{12}	R_5^3	r_6^2	r_4	1	R_2^2	r_7	r_{10}	R_3^3	R_6^3	R_4	r_3^2	R_1^3	R_6^4	R_4^3	R_3^3	i_3	r_8^2
R_5^3	r_{10}	i_{10}	r_4^2	i_{15}	R_5^4	r_5^2	i_{11}	r_1	i_6	r_6	R_5^2	i_1	r_9	R_6^2	r_3^2	R_2^3	1	r_8^2	R_4^3	r_2	R_1^2	r_7	R_5	R_3^2	r_5	i_8	R_4^2	R_4	R_1^4
R_6^3	i_9	i_{13}	r_2^2	r_3^2	r_9	R_6^4	r_4^2	r_{10}	i_{10}	i_5	i_{14}	R_6^2	R_4^2	R_1^3	r_1^2	r_7^2	r_8	1	r_5^2	r_6	R_5^2	R_3^3	R_2^3	R_6	R_5^2	R_2	R_4^3	R_3^3	
r_1	R_5^4	R_5^3	r_5^2	i_{11}	R_4	R_4^2	i_{12}	r_2	R_1^3	R_1^4	i_6	r_6	R_6^4	i_{10}	R_2^2	r_5	R_3	i_4	r_2^2	R_6^2	i_7	R_4^4	r_6^2	R_3^3	r_1^2	R_3^4	i_9	r_9^2	R_6
r_2	R_4	r_1	R_4^2	i_{12}	r_9^2	i_9	i_{13}	R_6^2	r_3	R_6	R_1^3	R_1^4	R_2	R_5^3	i_8	r_1^2	R_3^2	r_9	r_3^2	i_{10}	R_3^2	R_5	i_2	R_4^3	R_1^2	r_2^2	R_6^3	i_5	r_{10}^2
r_3	R_6	R_1^4	r_2	R_1^3	R_6^2	i_{13}	i_7	i_{14}	R_2^3	r_4	r_7	R_4^2	R_3	R_5^4	R_4^2	i_6	i_5	r_2^2	r_7^2	r_4^2	i_8	R_5^2	R_3^3	R_4^2	i_2	R_1^2	r_3^2	R_6^3	i_{10}
r_4	r_{10}^2	R_6	R_6^2	r_3	i_{10}	i_{14}	R_2^3	i_{15}	r_5	R_5^2	R_4^2	R_5	R_3^3	R_4	i_9	R_1^3	r_{10}	r_3^2	i_3	r_5^2	R_4^3	i_6	R_4^3	R_1	r_7	i_7	R_2^2	r_4^2	R_5^3
r_5	R_5^2	R_5	r_4	R_4^2	i_{15}	R_3^2	r_8	i_8	R_4^3	i_{11}	R_4^4	r_1^2	i_1	R_3	R_6^3	R_1^4	r_4^2	i_7	R_3^3	r_8^2	i_9	r_1	R_4^6	R_1^2	R_4^3	r_7	i_3	R_2^2	r_5^2
r_6	R_4^3	r_{10}	R_4^5	R_5^3	R_1^4	r_1	i_6	R_1^3	i_2	r_7	i_1	R_3^3	R_4^4	R_6^3	R_2	i_{15}	R_6	R_2^4	r_1^2	i_{13}	r_7^2	R_2^3	r_{10}^2	i_4	R_5^2	i_{11}	i_{12}	r_2	r_3
r_7	R_2^4	R_3^4	R_1^4	r_6	r_3	R_1^3	i_2	i_7	i_3	R_2^3	R_3^3	r_8	R_5	R_4^6	R_4	R_3^5	R_6^2	i_{12}	r_6^2	r_3^2	r_8^2	i_{15}	i_5	R_4^3	i_1	i_6	R_1^2	i_{13}	i_{14}
r_8	r_5	R_4^4	R_2^4	R_3^4	R_2^3	r_7	R_3^3	i_3	i_4	i_8	r_9	R_3^4	R_5^2	R_1	R_6	R_5^4	i_{14}	R_1^3	i_1	r_7^2	r_9^2	r_5^2	R_6^3	i_{12}	r_{10}	r_6	i_2	i_7	R_2^2
r_9	R_3^4	r_2^2	R_4^4	R_6^4	r_8	R_4^3	r_{10}	R_3^3	i_5	i_4	R_6^3	i_9	i_{11}	R_1^2	R_5	R_2	R_2^3	R_1^4	R_5^3	i_2	r_{10}^2	r_8^2	i_{14}	r_2	r_4^2	R_5^4	r_6	r_7	i_3
r_{10}	r_9	R_5^3	R_6^4	r_4^2	R_4^4	R_5^4	R_5^3	r_6	i_1	R_3^3	i_{10}	i_5	R_2^4	i_{13}	R_1	R_2^2	R_2^4	R_4	i_{11}	R_3^3	r_6^2	i_3	r_4	r_9^2	i_{15}	r_5^2	r_1	R_1^4	r_7
r_1^2	i_6	r_6^2	R_5^2	R_5	i_{11}	r_5	R_4^4	R_3^4	r_2^2	i_{12}	R_1	R_1^2	r_6	R_3^2	i_{10}	R_6	r_5^2	R_3^2	R_4^3	i_4	R_6^3	r_2	R_2	i_7	1	R_4^2	r_8	i_8	R_4^2
r_2^2	i_{12}	R_1^2	r_1^2	R_1	R_4^3	R_4^4	R_4^6	r_9	R_6^3	i_9	r_3^2	i_{13}	r_1	i_2	R_5^2	R_3	i_8	R_4^2	R_5^4	R_3^3	i_{10}	r_9^2	R_2^2	r_3	R_2	1	R_4^3	r_8	i_4
r_3^2	i_{13}	i_7	R_1^2	r_7^2	r_2^2	R_1	R_2	R_4^6	r_4^2	R_6^3	R_2^2	i_{14}	r_2	r_7	i_6	R_3^2	R_4^3	R_5	R_4	R_5^4	R_5^3	i_5	i_8	r_4	r_8^2	R_3	1	R_4^4	r_9
r_4^2	R_6^3	i_{14}	r_3^2	R_2^2	R_6^4	R_2	r_5^2	R_5^4	R_5^3	r_{10}	i_{15}	i_{10}	i_9	r_3	R_1^4	i_1	i_{12}	R_4^4	r_2^3	r_7	R_5^4	i_{15}	i_6	R_5	r_7^2	r_3	R_4	i_{14}	r_4^2	R_5^3
r_5^2	r_4	i_{15}	R_2^2	i_8	R_2	r_8^2	R_4^2	R_4	r_1	R_5^4	i_{11}	R_5^3	R_6^2	r_4	i_7	R_1	R_3^2	i_9	R_6	R_1^3	R_3^3	r_1^2	i_1	R_4^3	i_4	r_9^2	R_3	1	
r_6^2	i_2	R_3^2	i_1	r_{10}^2	i_6	R_5^2	R_5	r_1^2	R_1	R_1^2	R_3	r_7^2	r_7	i_4	r_{10}	R_6^2	r_1	i_{15}	R_2^4	R_3^4	R_6^4	i_{13}	R_4	R_2^2	R_6	r_4	r_5	i_{11}	i_{12}
r_7^2	i_7	i_3	i_2	R_3^2	R_1^2	r_6^2	R_3	R_1	R_2	r_3^2	r_8^2	R_2^2	r_3	r_8	r_6	i_5	i_{12}	R_5^2	R_6	R_4^4	R_5^4	R_6^3	R_4^2	i_{15}	r_9^2	r_{10}^2	R_5	r_1^2	r_2^2
r_8^2	R_2^2	i_8	i_3	i_4	r_7^2	R_3^2	r_9^2	R_3	R_4	R_2	R_4^2	r_5^2	i_{14}	r_5	r_7	r_9	R_1^2	i_1	R_6^2	R_5	R_1^4	R_6^4	i_{12}	R_5^3	i_9	i_5	r_{10}^2	r_6^2	R_1
r_9^2	r_8^2	R_4^2	i_4	i_9	R_3^2	i_5	R_6^2	r_{10}^2	R_6	R_3	r_2	R_4	R_2^2	i_{11}	r_8	r_2^2	i_2	r_{10}	i_{14}	R_5^2	R_4^2	R_1	R_3^4	R_4^5	i_{13}	R_6^3	i_{10}	i_1	r_6^2
r_{10}^2	R_3^2	r_9^2	i_5	R_6^2	i_1	i_{10}	r_4	R_5^2	R_5	r_6^2	R_6	R_3	i_3	R_4^2	r_9	i_{13}	r_6	r_4^2	R_3^2	i_{11}	R_4^4	R_1^2	R_1^4	R_2	r_3	i_{14}	i_{15}	R_5^3	i_6
i_1	R_3^3	i_5	r_{10}	i_{10}	r_6	R_5^3	R_5^2	i_6	r_6^2	i_2	r_{10}^2	R_3^2	r_8	i_9	R_6^4	i_{14}	R_1^4	r_5^2	r_5	i_{12}	R_1	i_7	R_6	r_8^2	r_4	i_{15}	i_{11}	r_1	R_3^1
i_2	r_7	R_3^3	r_6	i_1	R_3^1	i_6	r_6^2	R_1^2	r_7^2	i_7	R_3^2	i_3	R_4^2	r_9	R_4^5	i_{10}	r_2	i_{11}	R_5	r_2^2	R_2	i_{14}	r_9^2	i_8	r_{10}^2	R_5^2	r_1^2	i_{12}	i_{13}
i_3	R_2^3	r_8	r_7	R_3^3	i_7	i_2	R_2^3	r_7^2	r_8^2	R_2^2	i_4	i_8	r_4	R_4^4	R_1^4	r_{10}	i_{13}	i_6	r_{10}^2	R_1	R_4	r_4^2	i_9	i_{11}	i_5	i_1	r_6^2	R_1^2	r_3^2
i_4	i_8	R_4^3	r_8	r_9	i_3	R_3^3	i_5	R_5^3	r_9^2	r_8^2	i_9	R_4^2	i_{15}	r_1^2	R_4^2	R_4^6	i_7	r_6	i_{10}	r_6^2	R_6	R_2	i_{13}	r_1	R_6^3	r_{10}	i_1	i_2	r_7^2
i_5	i_4	i_9	r_9	R_6^2	R_3^2	r_{10}	i_{10}	i_1	r_{10}^2	R_3^2	R_6^2	r_9^2	i_8	i_{12}	R_4^4	r_3^2	r_7	R_5^4	i_{15}	i_6	R_5	r_7^2	r_3	R_4	i_{14}	r_4^2	R_5^3	r_6	i_2
i_6	r_6	i_1	R_5^3	R_5^2	r_1	i_{11}	r_1^2	i_{12}	R_1^2	R_1^3	r_6^2	i_2	R_4^3	i_5	r_4^2	r_4	R_4	i_8	R_4^4	i_9	r_3^2	r_3	R_3	i_3	R_5	r_5	R_4^2	R_4^2	r_2
i_7	r_3	r_7	R_1^3	i_2	i_{13}	R_1^2	r_7^2	r_3^2	R_2^2	i_{14}	i_3	R_2^3	R_6	R_4^3	r_1	i_1	i_9	r_1^2	R_3	R_6^4	r_5^2	i_{10}	i_4	r_5	R_3^2	r_6^2	R_1	r_2^2	R_6^3
i_8	i_{15}	r_5	R_2^3	r_8	R_2^2	i_3	i_4	r_8^2	R_4^2	r_5^2	R_4^3	i_{11}	i_{10}	R_5	r_3	R_4^3	r_3^2	i_2	i_5	R_3	r_2	R_5^4	r_2^2	i_6	r_9	R_3^3	R_2^3	r_7^2	R_2
i_9	R_4^2	i_{12}	R_4^3	r_2^2	i_4	r_9	R_6^3	i_5	R_6^2	r_9^2	i_{13}	r_2	r_5^2	i_6	r_5	R_1	i_3	R_3^4	r_4^2	i_1	r_4	R_3	i_7	R_4^1	r_3^2	R_6^4	r_{10}	R_3^3	R_5^2
i_{10}	i_5	R_6^2	R_6^3	i_{14}	r_{10}	r_4^2	i_{15}	R_5^3	R_5^2	i_1	r_4	r_{10}^2	i_4	r_2	r_2^2	i_7	R_4^3	R_2	i_8	r_1	r_1^2	i_2	R_4^2	R_3	R_2^2	R_2^2	r_5^2	R_5^4	r_6
i_{11}	R_5^3	R_5^2	i_{15}	r_5	r_5^2	i_8	R_4^3	R_4^2	i_{12}	r_1	r_1^2	i_6	r_{10}	r_{10}^2	i_{14}	R_4^2	R_2	i_3	r_9	r_9^2	i_{13}	R_1^4	R_1	i_2	R_4^4	r_8	i_4	r_8^2	R_4
i_{12}	r_1	i_6	i_{11}	r_1^2	R_4^2	R_4^3	r_2^2	i_9	i_{13}	r_2	R_1^2	R_1^3	R_4^5	i_1	i_{15}	R_5	r_8^2	r_8	R_6^4	i_5	i_{14}	R_6	r_7^2	r_7	R_1	R_4^4	r_9	i_4	r_9^2
i_{13}	r_2	R_3^3	i_{12}	R_1^2	i_9	r_2^2	r_3^2	R_6^3	i_{14}	R_6^2	i_7	r_3	R_4	r_6	i_{11}	r_6^2	i_4	R_4^4	R_2	r_{10}	i_{15}	r_{10}^2	i_3	R_2^4	r_7^2	R_1	R_6^4	r_9	i_5
i_{14}	R_6^2	r_3	i_{13}	i_7	R_6^3	r_3^2	R_2^2	r_4^2	i_{15}	i_{10}	R_2^3	r_4	r_9^2	R_1^4	i_{12}	i_2	r_9	R_1	r_8^2	R_5^4	i_{11}	i_1	r_8	R_5	i_3	r_7^2	R_2	R_6^4	r_{10}
i_{15}	i_{10}	r_4	i_{14}	R_2^3	r_4^2	R_2^2	i_8	r_5^2	i_{11}	R_5^3	r_5	R_5^2	i_5	R_6	i_{13}	r_7	R_6^4	r_7^2	i_4	R_4	i_{12}	r_6	R_4^4	r_6^2	r_8	i_3	r_8^2	R_2	R_5^4

FIG. 5. Multiplication table of the icosahedral rotation group I.

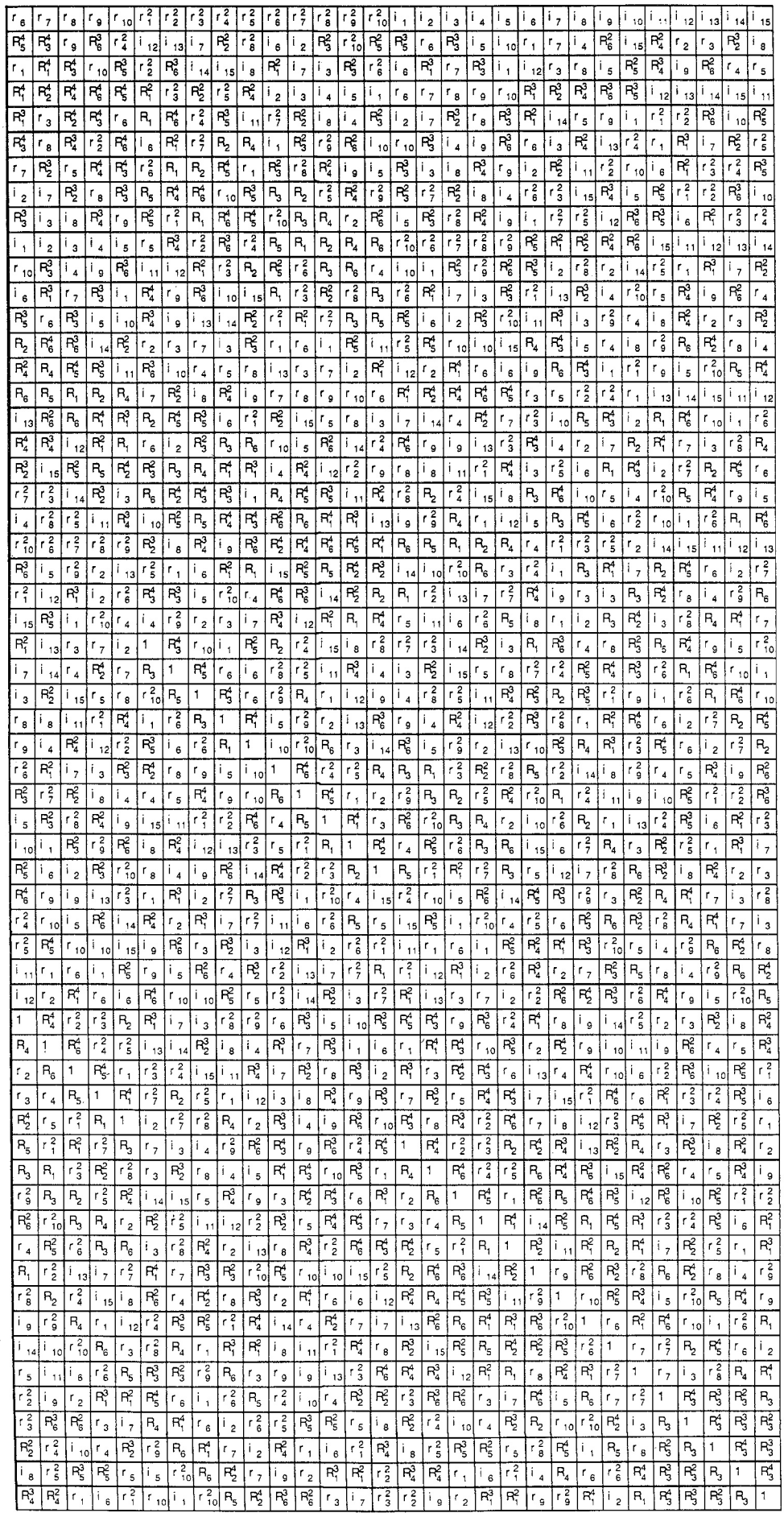

FIG. 5 (*continued*).

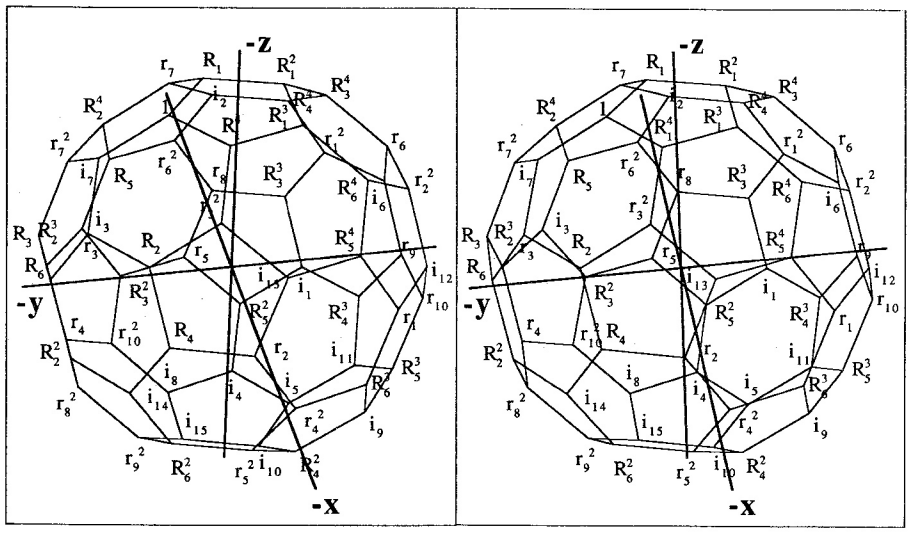

FIG. 6. Icosahedral vertex labels and the body-fixed x, y, and z axes.

generated by selecting a set of body-fixed coordinate axes whose origin is located at the center of the buckyball model. Icosahedral rotation operators represented in this basis from an icosahedral T_1 vector irreducible representation (irrep). Using the icosahedral T_1 vector irreps as rotation matrices in R^3, a radial lab-fixed vector,

$$\vec{\mathrm{A}} = \vec{1\mathrm{A}},$$

chosen to pass through a buckyball vertex, may be rotated to another vertex,

$$D^{T_1}\{g\}\vec{\mathrm{A}} = D^{T_1}\{g\}\vec{1\mathrm{A}} = \vec{g1\mathrm{A}} = \vec{g\mathrm{A}}. \tag{3.1}$$

where $D^{T_1}(g)$ is the 3×3 T_1 irrep. Each new radial vector $\vec{g\mathrm{A}}$ is labeled with the icosahedral group operator g that generated it. By using the 60 proper rotations of the icosahedral group a labeled radial vector may be sent to each of the 60 buckyball vertices. The group operator g also labels the vertex through which the vector $\vec{g\mathrm{A}}$ passes. The improper rotations of the icosahedral group will only interchange the radial vectors and will not generate anything new. Thus, the 60 radial vectors $\vec{g\mathrm{A}}$ are all that can be made from $\vec{1\mathrm{A}}$ using icosahedral operations, and together they form a radial orbit labeled A. Icosahedral vertex labels and body-fixed axes used to make the radial A orbit are shown in Fig. 6.

A second orbit of 120 tangential vectors is generated using the same technique with the full icosahedral group I_h. This time an initial vector $\vec{1\mathrm{B}}$ is chosen perpendicular to $\vec{1\mathrm{A}}$ and 45° away from the σ_5 reflection plane as shown in Fig. 7. Upon σ_5 reflection a new vector $\vec{\sigma_5\mathrm{B}}$ is generated from the initial vector $\vec{1\mathrm{B}}$, 45° on the other side of the σ_5 reflection plane. This completes the right-handed orthogonal coordinate triad located at the vertex labeled by the unit operator. The remaining I_h operators are used to complete the tangential orbit labeled B. The z and x axes of each coordinate system belong to orbits A and B, respectively, and are labeled by the proper icosahedral rotation of the corresponding vertex. The y axes belong to the B orbit and are labeled with improper icosahedral rotations. The label of any y axis is obtained by computing the group product between the vertex label of the y axis, and σ_5. Together, the 60-element radial orbit A, generated by the icosahedral rotation group I, and the 120-element tangential orbit B, generated by the full-

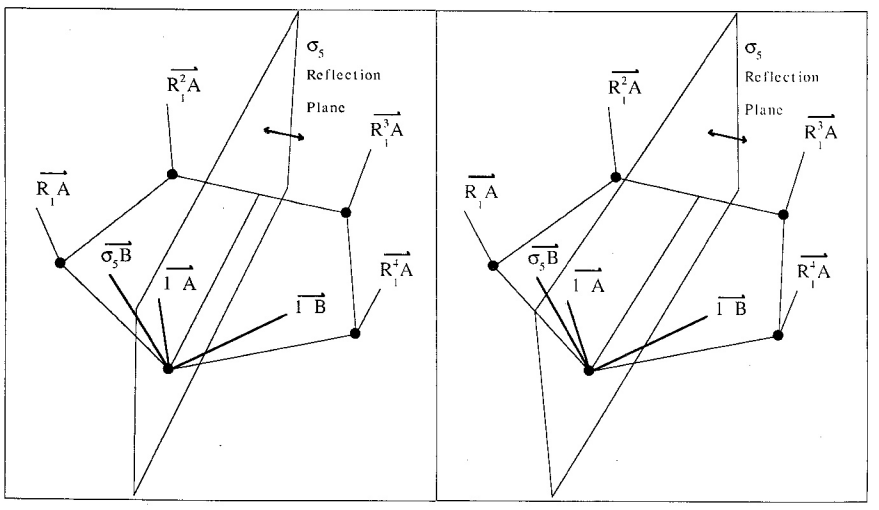

FIG. 7. Orientation and labeling of the symmetrically defined coordinate axes located at the unit vertex. The σ_5 reflection plane used to reflect $1B$ into $\sigma_5 B$ is illustrated.

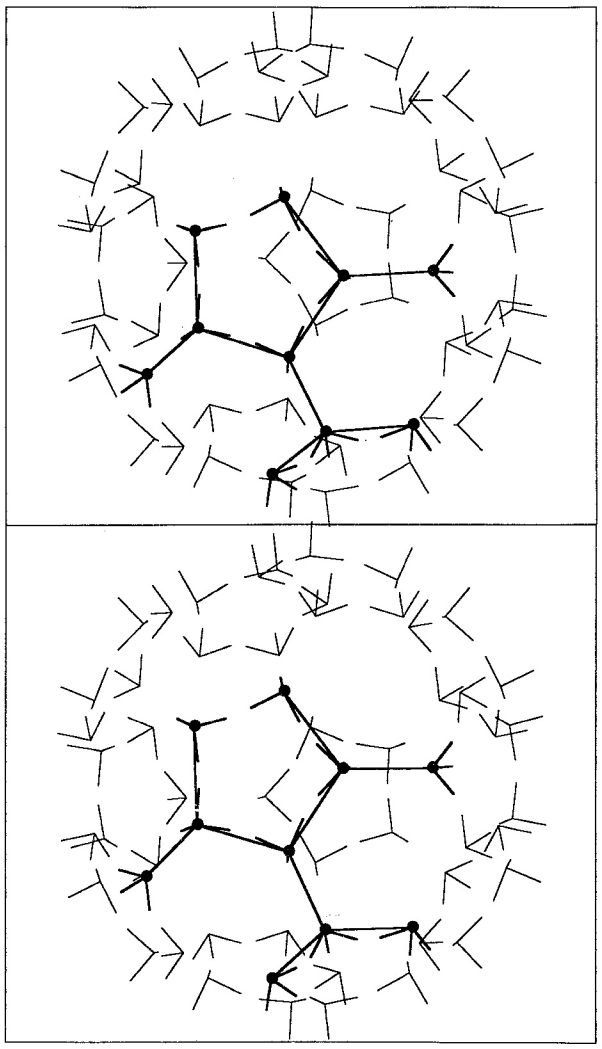

FIG. 8. The 60 symmetrically defined orthogonal coordinate traids of buckyball. The unit cell used to calculate force matrix elements is highlighted.

icosahedral group I_h, are shown in Fig. 8, and form a set of 180 coordinate vectors that corresponds to the 3×60 degrees of freedom of the 60 carbon atoms.

The vectors of the orbits A and B correspond to state vectors generated by group operators,

$$D^{T_1}\{g\}\quad \vec{O} = gO \quad \leftrightarrow \quad g|O\rangle = |gO\rangle\ ,$$

where O is the orbit label A or B. The state $|gO\rangle$ represents the displacement from equilibrium, of a single mass located at the vertex labeled by g, in the direction $\overrightarrow{gO}$. These 180 state vectors form a complete set, within which any distortion of the buckyball spring-mass model can be expressed as a linear combination. In order to determine the expansion coefficients of the $|gO\rangle$ that yield normal modes, Newton's 2nd law is expressed in the $|gO\rangle$ basis,

$$\frac{d^2}{dt^2}|\psi\rangle = -\mathbf{M}^{-1}\mathbf{K}|\psi\rangle\ ,$$

$$\frac{d^2}{dt^2}\langle gO|\psi\rangle = -\sum_{g',O'}\langle gO|\mathbf{M}^{-1}\mathbf{K}|g'O'\rangle\langle g'O'|\psi\rangle \quad (3.2)$$

$$= \frac{-1}{m_c}\sum_{g',O'}\langle gO|\mathbf{K}|g'O'\rangle\langle g'O'|\psi\rangle\ .$$

The mass operator $\mathbf{M}$, in the $|gO\rangle$ basis, is diagonal with all elements equal to the mass of the carbon atom m_c. The force constant operator $\mathbf{K}$ couples the state vectors $|gO\rangle$ for a total of 180 coupled differential equations. Columns of the transformation matrix that diagonalize the force contant matrix, contain the expansion coefficients of the normal modes of vibration in terms of the $|gO\rangle$ basis. Corresponding elements of the diagonalized force matrix are the vibrational eigenfrequencies squared.

Prior to diagonalization, the force matrix elements $\langle gO|\mathbf{K}|g'O'\rangle$ are force constants that determine the force on the mass at the gth vertex in the $\overrightarrow{gO}$ direction when the mass at the g'th vertex is displaced in the $\overrightarrow{g'O'}$ direction. These constants depend on the geometry of buckyball, and the springs used to model the covalent bonds. Two springs, with spring constants p and h, are used to model the stretching of the single and double bonds along the pentagonal and hexagonal edges. Two additional springs with spring constants π and η, are used to model the bending of the single and double bonds. The spring constants p, h, π, and η are the only parameters of the model that can be adjusted. By setting certain spring constants to zero it is possible to check special test cases of reduced symmetry for which analytic results are

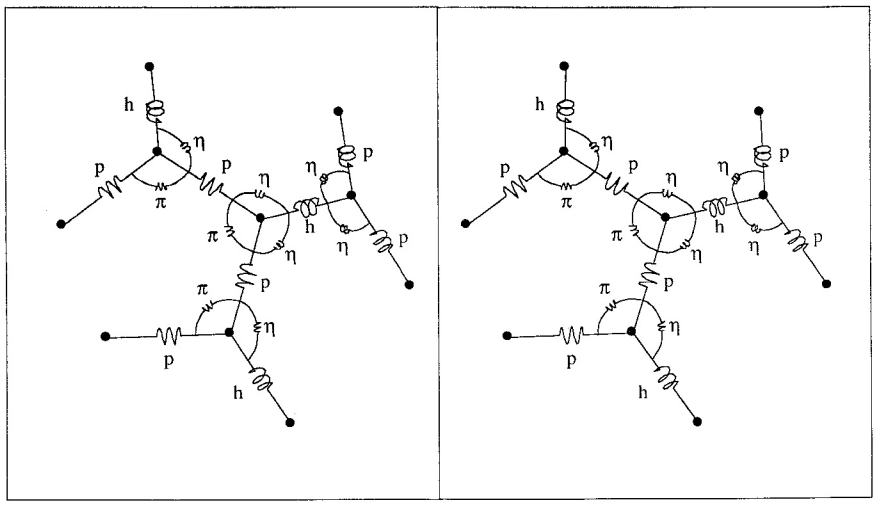

FIG. 9. The springs of the unit cell highlighted in Fig. 8. Single-bond parameters are p and π. Double-bond parameters are h and η.

available. These test cases are examined in Sec. VI. A unit cell illustrating the relative position of the different springs is shown in Fig. 9. The stretching springs couple nearest neighbors, and the bending springs couple nearest and next-nearest neighbors for a total of 10 masses and 30 coordinates in the unit cell. Each coordinate is labeled gA, gB, or $g\sigma_5 B$, and corresponds to the displacement of the mass at the gth vertex in the $\overrightarrow{gA}$, $\overrightarrow{gB}$, or $\overrightarrow{g\sigma_5 B}$ directions. The potential energy of the unit cell is determined as a function of these coordinates and the elements of the force matrix are the second-order derivatives of this potential.

The potential energy may be split into a stretching component and a bending component,

$$V_s = \{\tfrac{1}{2}h(1-|\vec{\mathbf{c}}|)^2 + \tfrac{1}{2}p[(1-|\vec{\mathbf{a}}|)^2 + (1-|\vec{\mathbf{b}}|)^2]\}, \tag{3.2a}$$

$$\begin{aligned} V_b = (&\tfrac{1}{2}\pi\{[\Theta-\theta(1)]^2 + [\Theta-\theta(R_1)]^2 \\ &+ [\Theta-\theta(R_1^4)]^2\} + \tfrac{1}{2}\eta\{[\Phi-\phi(1)]^2 \\ &+ [\Phi-\phi(R_1)]^2 + [\Phi-\gamma(R_1^4)]^2 \\ &+ [\Phi-\gamma(1)]^2 + [\Phi-\phi(i_7)]^2 + [\Phi-\gamma(i_7)]^2\}), \end{aligned} \tag{3.3b}$$

$$V = V_s + V_b . \tag{3.3c}$$

To determine the functional form of the potential, arbitrary displacement vectors $\overrightarrow{d(g)}$ are represented in the body-fixed axes. The vectors $\overrightarrow{d(g)}$ are displacements from equilibrium of the masses of the unit cell labeled with group operators g, and are illustrated in Fig. 10. Edge vectors $\vec{\mathbf{a}}, \vec{\mathbf{b}}, \ldots, \vec{\mathbf{n}}$ are determined by the vector sum of the corresponding equilibrium edge vector $\hat{\mathbf{a}}, \hat{\mathbf{b}}, \ldots, \hat{\mathbf{n}}$, minus the displacement vector $\overrightarrow{d(g)}$ from which the edge vector originates, plus the displacement vector at which the edge vector terminates. For example, the edge vector $\vec{\mathbf{a}}$ is given by

$$\vec{\mathbf{a}} = \hat{\mathbf{a}} - \overrightarrow{d(1)} + \overrightarrow{d(R_1^4)} .$$

The equilibrium edge vectors $\hat{\mathbf{a}}, \hat{\mathbf{b}}, \ldots, \hat{\mathbf{n}}$ correspond to the edge vectors $\vec{\mathbf{a}}, \vec{\mathbf{b}}, \ldots, \vec{\mathbf{n}}$ when the displacements $\mathrm{d}(g)$ are zero, and are defined to be of unit length. Deviations from unit length of an edge determine how much a stretching spring along the edge has been compressed or extended. This change in length is squared and multiplied by one-half the corresponding spring constant, and determines the contribution of the particular stretching spring to the potential. For example, the hexagonal stretching spring, with spring constant h, along edge c in Figs. 9 and 10, will contribute the first term in Eq. (3.3a),

$$\begin{aligned} V_c &= \tfrac{1}{2}h\{|\hat{\mathbf{c}}| - |\vec{\mathbf{c}}|\}^2 \\ &= \tfrac{1}{2}h\{1 - |\vec{\mathbf{c}}|\}^2 . \end{aligned}$$

The pentagonal stretching springs along the edges a and b contribute the remainder of the stretching potential.

The edge vectors $\vec{\mathbf{a}}, \vec{\mathbf{b}}, \ldots, \vec{\mathbf{n}}$ are also used to calculate the angles $\theta(g), \phi(g)$, and $\gamma(g)$ shown in Fig. 10. When the displacement vectors $\overrightarrow{d(g)}$ are all zero, the angles $\theta(g)$, $\phi(g)$, and $\gamma(g)$ have equilibrium values $\Theta = 108°$, $\Phi = 120°$, and $\Phi = 120°$, respectively. Upon distortion of the unit cell, these angles will change, compressing or expanding the bending springs shown in Fig. 9. The values of the angles $\theta(g), \phi(g)$, and $\gamma(g)$ are calculated from the arcosine of the normalized scalar product between selected edge vectors. For example, the value of $\theta(1)$ is given by

$$\theta(1) = \arccos\left\{\frac{\vec{\mathbf{a}}\cdot\vec{\mathbf{b}}}{|\vec{\mathbf{a}}||\vec{\mathbf{b}}|}\right\} .$$

The differences between the equilibrium angles Θ and Φ, and the distorted angles $\theta(g), \phi(g)$, and $\gamma(g)$ are squared and multiplied by one-half the corresponding spring constant, to obtain the bending potential energy. For example, the first term in Eqs. (3.3b) is the potential energy of the pentgonal bending spring π that spans the angle $\theta(1)$, and is given by

$$V_{\theta(1)} = \tfrac{1}{2}\pi[\Theta - \theta(1)]^2 ,$$

where the radius of curvature of the spring is included in the spring constant. The remaining bending springs contribute the rest of the bending potential.

The edge vectors $\vec{\mathbf{a}}, \vec{\mathbf{b}}, \ldots, \vec{\mathbf{n}}$ are functions of the displacement vectors $\overrightarrow{d(g)}$. Each of the 10 $\overrightarrow{d(g)}$ are represented in terms of the x, y, and z axes of the body-fixed coordinate system, and have 30 corresponding components $x(g)$, $y(g)$, and $z(g)$. The potential energy is Eq. (3.3) will be a function

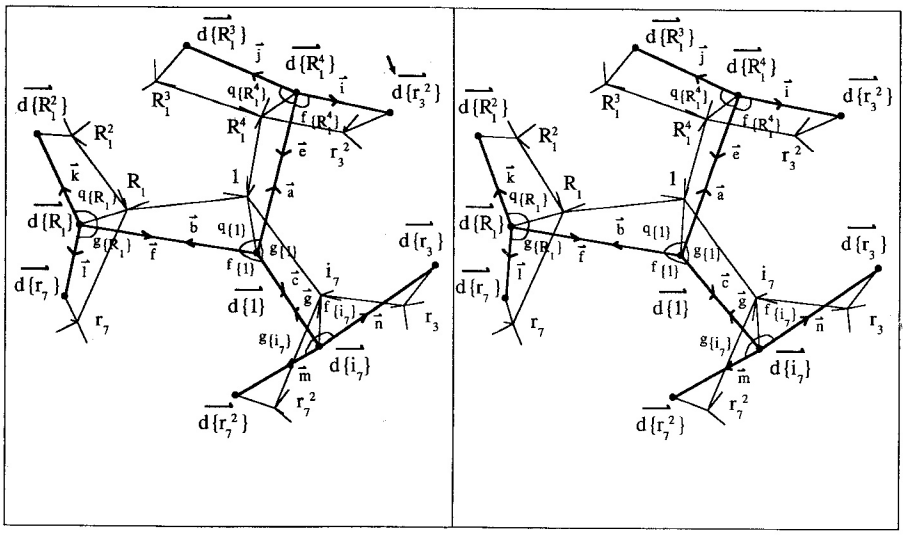

FIG. 10. Stereoscopic view of an arbitrarily distorted unit cell. Vectors and angles used to calculate the potential are labeled. An undistorted unit cell is shown for reference. Group operator defined coordinate systems of the unit cell are included.

TABLE I. Nonzero elements of the $\langle 1A|$ and $\langle 1B|$ rows of the initial force matrix as a function of spring constants p, h, π, and η.

$\langle 1A\|\mathbf{K}\|1A\rangle$	$=(0.081426)p$	$+(0.040713)h$	$+(0.462764)\pi$	$+(1.46566)\eta$	$\langle 1A\|\mathbf{K}\|r_3A\rangle$	$=(0)p+(0)h+(0)\pi$	$+(0.122138)\eta$
$\langle 1A\|\mathbf{K}\|1B\rangle$	$=-(0.157533)p$	$+(0.139741)h$	$-(0.895307)\pi$	$+(1.09754)\eta$	$\langle 1A\|\mathbf{K}\|r_3B\rangle$	$=(0)p+(0)h+(0)\pi$	$+(0.085289)\eta$
$\langle 1A\|\mathbf{K}\|\sigma_5B\rangle$	$=-(0.157533)p$	$+(0.139741)h$	$-(0.895307)\pi$	$+(1.09754)\eta$	$\langle 1A\|\mathbf{K}\|\rho_r^3B\rangle$	$=(0)p+(0)h+(0)\pi$	$+(0.316143)\eta$
$\langle 1A\|\mathbf{K}\|i_7A\rangle$	$=(0)p$	$+(0.040713)h$	$+(0)\pi$	$-(0.977107)\eta$	$\langle 1A\|\mathbf{K}\|r_3^2A\rangle$	$=(0)p+(0)h+(0)\pi$	$+(0.122138)\eta$
$\langle 1A\|\mathbf{K}\|i_7B\rangle$	$=(0)p$	$+(0.139741)h$	$+(0)\pi$	$-(0.294679)\eta$	$\langle 1A\|\mathbf{K}\|r_3^2B\rangle$	$=(0)p+(0)h+(0)\pi$	$-(0.248647)\eta$
$\langle 1A\|\mathbf{K}\|\sigma_{11}B\rangle$	$=(0)p$	$+(0.139741)h$	$+(0)\pi$	$-(0.294679)\eta$	$\langle 1A\|\mathbf{K}\|\rho_5^2B$	$=(0)p+(0)h+(0)\pi$	$+(0.213062)\eta$
$\langle 1A\|\mathbf{K}\|R_1^4A\rangle$	$=(0.040713)p$	$+(0)h$	$-(0.308510)\pi$	$-(0.488553)\eta$	$\langle 1A\|\mathbf{K}\|R_1^3A\rangle$	$=(0)p+(0)h+(0.077127)\pi$	$+(0)\eta$
$\langle 1A\|\mathbf{K}\|R_1^4B\rangle$	$=(0.036660)p$	$+(0)h$	$+(0.827726)\pi$	$-(1.16149)\eta$	$\langle 1A\|\mathbf{K}\|R_1^3B\rangle$	$=(0)p+(0)h-(0.264645)\pi$	$+(0)\eta$
$\langle 1A\|\mathbf{K}\|\sigma_4B\rangle$	$=-(0.194194)p$	$+(0)h$	$+(0.366017)\pi$	$-(0.007219)\eta$	$\langle 1A\|\mathbf{K}\|\sigma_8B\rangle$	$=(0)p+(0)h-(0.033791)\pi$	$+(0)\eta$
$\langle 1A\|\mathbf{K}\|R_1A\rangle$	$=(0.040713)p$	$+(0)h$	$-(0.308510)\pi$	$-(0.488553)\eta$	$\langle 1A\|\mathbf{K}\|R_1^2A\rangle$	$=(0)p+(0)h+(0.077127)\pi$	$+(0)\eta$
$\langle 1A\|\mathbf{K}\|R_1B\rangle$	$=-(0.194194)p$	$+(0)h$	$+(0.366017)\pi$	$-(0.007219)\eta$	$\langle 1A\|\mathbf{K}\|R_1^2B\rangle$	$=(0)p+(0)h-(0.33791)\pi$	$+(0)\eta$
$\langle 1A\|\mathbf{K}\|\sigma_{10}B\rangle$	$=(0.036660)p$	$+(0)h$	$+(0.827726)\pi$	$-(1.16149)\eta$	$\langle 1A\|\mathbf{K}\|\sigma_{15}B\rangle$	$=(0)p+(0)h-(0.264645)\pi$	$+(0)\eta$
$\langle 1A\|\mathbf{K}\|r_7^2A\rangle$	$=(0)p$	$+(0)h$	$+(0)\pi$	$+(0.122138)\eta$	$\langle 1A\|\mathbf{K}\|r_7A\rangle$	$=(0)p+(0)h+(0)\pi$	$+(0.122138)\eta$
$\langle 1A\|\mathbf{K}\|r_7^2B\rangle$	$=(0)p$	$+(0)h$	$+(0)\pi$	$+(0.316143)\eta$	$\langle 1A\|\mathbf{K}\|r_7B\rangle$	$=(0)p+(0)h+(0)\pi$	$+(0.213062)\eta$
$\langle 1A\|\mathbf{K}\|\rho_5^3B\rangle$	$=(0)p$	$+(0)h$	$+(0)\pi$	$+(0.085289)\eta$	$\langle 1A\|\mathbf{K}\|\rho_4^2B\rangle$	$=(0)p+(0)h+(0)\pi$	$-(0.248647)\eta$
$\langle 1B\|\mathbf{K}\|1A\rangle$	$=-(0.157533)p$	$+(0.139741)h$	$-(0.895307)\pi$	$+(1.09754)\eta$	$\langle 1B\|\mathbf{K}\|r_3A\rangle$	$=(0)p+(0)h+(0)\pi$	$-(0.248646)\eta$
$\langle 1B\|\mathbf{K}\|1B\rangle$	$=(0.959287)p$	$+(0.479644)h$	$+(2.07763)\pi$	$+(4.26717)\eta$	$\langle 1B\|\mathbf{K}\|r_3B\rangle$	$=(0)p+(0)h+(0)\pi$	$-(0.173629)\eta$
$\langle 1B\|\mathbf{K}\|\sigma_5B\rangle$	$=-(0.349730)p$	$+(0.479644)h$	$+(1.38665)\pi$	$-(1.84158)\eta$	$\langle 1B\|\mathbf{K}\|\rho_4^3B\rangle$	$=(0)p+(0)h+(0)\pi$	$-(0.643597)\eta$
$\langle 1B\|\mathbf{K}\|i_7A\rangle$	$=(0)p$	$+(0.139741)h$	$+(0)\pi$	$-(0.294679)\eta$	$\langle 1B\|\mathbf{K}\|r_3^2A\rangle$	$=(0)p+(0)h+(0)\pi$	$+(0.085289)\eta$
$\langle 1B\|\mathbf{K}\|i_7B\rangle$	$=(0)p$	$+(0.479644)h$	$+(0)\pi$	$+(2.72462)\eta$	$\langle 1B\|\mathbf{K}\|r_3^2B\rangle$	$=(0)p+(0)h+(0)\pi$	$-(0.173629)\eta$
$\langle 1B\|\mathbf{K}\|\sigma_{11}B\rangle$	$=(0)p$	$+(0.479644)h$	$+(0)\pi$	$-(2.511145)\eta$	$\langle 1B\|\mathbf{K}\|\rho_5^2B\rangle$	$=(0)p+(0)h+(0)\pi$	$+(0.148780)\eta$
$\langle 1B\|\mathbf{K}\|R_1^4A\rangle$	$=-(0.194194)p$	$+(0)h$	$+(0.366017)\pi$	$-(0.007219)\eta$	$\langle 1B\|\mathbf{K}\|R_1^3A\rangle$	$=(0)p+(0)h-(0.033791)\pi$	$+(0)\eta$
$\langle 1B\|\mathbf{K}\|R_1^4B\rangle$	$=-(0.174865)p$	$+(0)h$	$-(1.15476)\pi$	$+(0.053294)\eta$	$\langle 1B\|\mathbf{K}\|R_1^3B\rangle$	$=(0)p+(0)h+(0.115945)\pi$	$+(0)\eta$
$\langle 1B\|\mathbf{K}\|\sigma_4B\rangle$	$=(0.926276)p$	$+(0)h$	$-(0.261498)\pi$	$+(0.228144)\eta$	$\langle 1B\|\mathbf{K}\|\sigma_8B\rangle$	$=(0)p+(0)h+(0.014804)\pi$	$+(0)\eta$
$\langle 1B\|\mathbf{K}\|R_1A\rangle$	$=(0.036660)p$	$+(0)h$	$+(0.827726)\pi$	$-(1.16149)\eta$	$\langle 1B\|\mathbf{K}\|R_1^2A\rangle$	$=(0)p+(0)h-(0.264645)\pi$	$+(0)\eta$
$\langle 1B\|\mathbf{K}\|R_1B\rangle$	$=-(0.174865)p$	$+(0)h$	$-(1.15476)\pi$	$+(0.053294)\eta$	$\langle 1B\|\mathbf{K}\|R_1^2B\rangle$	$=(0)p+(0)h+(0.115945)\pi$	$+(0)\eta$
$\langle 1B\|\mathbf{K}\|\sigma_{10}B\rangle$	$=(0.033011)p$	$+0)h$	$-(2.04803)\pi$	$-(2.73959)\eta$	$\langle 1B\|\mathbf{K}\|\sigma_{15}B\rangle$	$=(0)p+(0)h+(0.908068)\pi$	$+(0)\eta$
$\langle 1B\|\mathbf{K}\|r_7^2A\rangle$	$=(0)p$	$+(0)h$	$+(0)\pi$	$+(0.213062)\eta$	$\langle 1B\|\mathbf{K}\|r_7A\rangle$	$=(0)p+(0)h+(0)\pi$	$+(0.316143)\eta$
$\langle 1B\|\mathbf{K}\|r_7^2B\rangle$	$=(0)p$	$+(0)h$	$+(0)\pi$	$+(0.551490)\eta$	$\langle 1B\|\mathbf{K}\|r_7B\rangle$	$=(0)p+(0)h+(0)\pi$	$+(0.551490)\eta$
$\langle 1B\|\mathbf{K}\|\rho_5^3B\rangle$	$=(0)p$	$+(0)h$	$+(0)\pi$	$+(0.148780)\eta$	$\langle 1B\|\mathbf{K}\|\rho_4^2B\rangle$	$=(0)p+(0)h+(0)\pi$	$-(0.643597)\eta$

of the $x(g)$, $y(g)$, and $z(g)$, which form an initial set of 30 generalized coordinates. These initial generalized coordinates are functions of the more useful set of group operator defined generalized coordinates gA, gB, and $g\sigma_5B$. The transformation between $x(g)$, $y(g)$, $z(g)$, and gA, gB, $g\sigma_5B$, is given by the icosahedral T_1 vector irreps $D^{T_1}(g)$. Once expanded in terms of the group operator variables gA, gB, and $g\sigma_5B$, the potential energy may be used to obtain force matrix elements. These elements will be the second-order partial derivatives of the potential energy, with respect to the generalized coordinates gA, gB, and $g\sigma_5B$,

$$\langle g\mathrm{O}|\mathbf{K}|g'\mathrm{O}'\rangle = \left|\frac{\partial^2}{\partial g\mathrm{O}\partial g'\mathrm{O}'}V(gA,gB,g\sigma_5B)\right|_{\text{equilibrium}} \tag{3.4}$$

A four-point central difference method was used to numerically calculate the second-order derivatives in Eq. (3.4) because the algebra of an analytic approach was prohibitive.

The force matrix elements in Eq. (3.4) are linear functions of the spring constants p, h, π, and η. The proportionality factors between spring constants and force matrix elements are determined by setting three of the four spring constants to 0 and the remaining constant to 1. A list of these porportionality factors between spring constants p, h, π, and η, and force matrix elements that couple $\langle 1A|$ and $\langle 1B|$ to the $|g\mathrm{O}\rangle$ of the unit cell, are given in Table I. These values permit the rapid calculation of the $\langle 1A|$ and $\langle 1B|$ rows of the force matrix, for any choice of spring constants. By construction, the force matrix commutes with all the group operators of I_h and therefore has icosahedral symmetry. Thus, it is possible to block the diagonalize the force matrix using icosahedral symmetry projection, which requires only the two force matrix rows $\langle 1A|$ and $\langle 1B|$.

IV. ICOSAHEDRAL SYMMETRY PROJECTION

In Sec. III, matrix elements of the force constant operator $\mathbf{K}$ were calculated in the 180-dimensional, group operator defined representation $|g\mathrm{O}\rangle$. The operator $\mathbf{K}$ commutes with all group operators of the full icosahedral group I_h,

$$g^{-1}\mathbf{K}g=\mathbf{K};\ \{g\in I_H\},$$

and therefore may be reduced using icosahedral symmetry projection. This reduction requires the first two rows of the initial force matrix and is affected by icosahedral symmetry projection operators P_{ij}^{α} defined by

$$P_{ij}^{\alpha}=\frac{l^{\alpha}}{{}^oG}\sum_{g\in G}D_{ij}^{\alpha *}(g)g\,. \tag{4.1}$$

In Eq. (4.1), α is the irrep label, ${}^oG$ is the order of the group, l^{α} is the dimension of the αth irrep, and $D_{ij}^{(\alpha)}(g)$ is the i,jth element of the αth irrep of g. Since Eq. (4.1) is a sum over

$I_h \updownarrow C_v$

	+	-
A_g	1	0
T_{1g}	1	2
T_{3g}	1	2
G_g	2	2
H_g	3	2
A_u	0	1
T_{1u}	2	1
T_{3u}	2	1
G_u	2	2
H_u	2	3

FIG. 11. The $I_h \supset C_v$ correlation table.

group operators, projection operators formally belong to the theory of rings.[22]

Operation on an initial state vector $|1O\rangle$ with projection operators defined by Eq. (4.1) will yield the group irreducible representation $|O_{ij}^{\alpha}\rangle$,

$$P_{ij}^{\alpha}|1O\rangle/\sqrt{N^{\alpha}} = |O_{ij}^{\alpha}\rangle = \left\{\frac{l^{\alpha}}{{}^{o}G}\right\}^{1/2} \sum_{g\in G} D_{ij}^{\alpha *}(g)|gO\rangle , \tag{4.2}$$

where $N^{\alpha} = l^{\alpha}/{}^{o}G$ is required for normalization. In the $|O_{ij}^{\alpha}\rangle$ basis, group operators will be block diagonal with group irreps forming the block diagonal elements. Operators that commute with all group operators will also be block diagonalized in this basis. Properties of the projection operators P_{ij}^{α}, and the irreducible basis vectors $|O_{ij}^{\alpha}\rangle$ are given in Appendix C.

The form of the block diagonalized force matrix in the $|O_{ij}^{\alpha}\rangle$ representation is determined by the local symmetry of the coordinate axes shown in Fig. 7. The vector $\overrightarrow{1A}$ is invariant under the operation of the + type projection operator P^{+} of the local symmetry group $C_V = \{1,\sigma_5\}$,

$$P^{+}\overrightarrow{1A} = \tfrac{1}{2}\{1+\sigma_5\}\overrightarrow{1A} = \overrightarrow{1A} .$$

This means that the frequency $f^{\alpha,+}$ with which the icosahedral irrep α will occur in the $|A_{ij}^{\alpha}\rangle$ representation of an icosahedral group operator is given by the + column of the $I_h \supset C_V$ correlation table shown in Fig. 11. This is schematically expressed as

$$A(g) = D^{A_g}(g) \oplus D^{T_{1g}}(g) \oplus D^{T_{3g}}(g) \oplus 2D^{G_g}(g) \oplus 3D^{H_g}(g) \oplus 2D^{T_{1u}}(g) \oplus 2D^{T_{3u}}(g) \oplus 2D^{G_u}(g) \oplus 3D^{H_u}(g) . \tag{4.3}$$

The local symmetry of the vector 1B is described by the trivial group $C_1 = \{1\}$. The first column of the I_h character table given in Appendix B determines the frequency $f^{\alpha,1} = l^{\alpha}$ of the αth irrep in the $|B_{ij}^{\alpha}\rangle$ representation,

$$B(g) = D^{A_g}(g) \oplus 3D^{T_{1g}}(g) \oplus 3D^{T_{3g}}(g) \oplus 4D^{G_g}(g) \oplus 5D^{H_g}(g) \oplus D^{A_u}(g) \oplus 3D^{T_{1u}}(g) \oplus 3D^{T_{3u}}(g) \oplus 4D^{G_u}(g) \oplus 5D^{H_u}(g) . \tag{4.4}$$

Together, Eqs. (4.3) and (4.4) determine the frequencies of the I_h irreps in the 180-dimensional buckyball space defined by orbits A and B.

$$A(g) \oplus B(g) = 2D^{A_g}(g) \oplus 4D^{T_{1g}}(g) \oplus 4D^{T_{3g}}(g) \oplus 6D^{G_g}(g) \oplus 8D^{H_g}(g) \oplus D^{A_u}(g) \oplus 5D^{T_{1u}}(g) \oplus 5D^{T_{3u}}(g) \oplus 6D^{G_u}(g) \oplus 7D^{H_u}(g) . \tag{4.5}$$

The block diagonal form of the force constant operator $\mathbf{K}$ in the $|O_{ij}^{\alpha}\rangle$ representation is obtained from Eq. (4.5) by interchaning the frequency of occurrence f^{α} of the αth irrep, with the dimension l^{α} of the αth irrep,

$$A(\mathbf{K}) \oplus B(\mathbf{K}) = K^{A_g} \oplus 3K^{T_{1g}} \oplus 3K^{T_{3g}} \oplus 4K^{G_g} \oplus 5K^{H_g} \oplus K^{A_u} \oplus 3K^{T_{1u}} \oplus 3K^{T_{3u}} \oplus 4K^{G_u} \oplus 5K^{H_u} . \tag{4.6}$$

The K^{α} in Eq. (4.6) are force matrix blocks with a dimension d_{α} given by the sum of $I_h \supset C_V$ correlation elements $f^{\alpha,+}$ and irrep dimension l^{α},

$$d_{\alpha} = f^{\alpha,+} + l^{\alpha} .$$

For example, there will be five identical 8×8 block diagonal elements in the icosahedrally projected force matrix labeled by the I_h irrep $\alpha = H_g$. The dimension $d_{H_g} = 8$ of the K^{H_g} blocks is the number of distinct H_g-type eigenvalues, and the frequency $l^{H_g} = 5$ of the K^{H_g} blocks is the degeneracy of the distinct H_g eigenvalues. A list of I_h irrep labels with the number of distinct eigenvalues per label, and degeneracies per eigenvalue is given in Table II. The form of the force matrix blocks are given in Fig. 12.

TABLE II. The number of distinct vibrational eigenvalues and degeneracies of buckyball determined by icosahedral irrep labels.

I_h group label	Number of eigenvalues	Degeneracy	
A_g	2	1	
T_{1g}	3	3	Even
T_{3g}	4	3	parity
G_g	6	4	
H_g	8	5	
A_u	1	1	
T_{1u}	4	3	Odd
T_{3u}	5	3	parity
G_u	6	4	
H_u	7	5	

V. RESULTS

Numerical diagonalization of the force matrix blocks shown in Fig. 12 will yield the vibrational eigenvalues of the spring mass model of buckyball. Diagonal elements $K_{ii}^{\alpha} = K_i^{\alpha}$ of the force matrix are effective spring constants of harmonic oscillators in normal coordinates with corresponding eigenfrequencies,

$$\omega_i^{\alpha} = \{K_i^{\alpha}/m_c\}^{1/2} .$$

The l^{α} force matrix blocks K^{α} are identical so it is redundant to diagonalize more than one to obtain the l^{α}-fold degenerate $i = 1,...,d_{\alpha}$ eigenfrequencies ω_i^{α}. As a result, the diagonalization of the original 180-dimensional force matrix is reduced by icosahedral symmetry projection, to the diagonalization of one 2×2, one 7×7, one 8×8, matrix, and two 4×4, two 5×5 and two 6×6 matrices. This greatly reduces the numerical labor required to calculate eigenfrequencies and permits the entire problem to be solved for any choice of spring constants in a few seconds on a small personal computer.

The functional dependence of the buckyball vibrational eigenfrequencies ω_i^{α} on the spring constants p, h, π, and η is displayed in the form of eigenvalue trajectories shown in Fig. 13. To make the trajectories, both stretching spring constants p and h are set equal to 1 in arbitrary units. Then the bending spring π and η are set equal to each other and varied simultaneously from 0 to 1. For each value of $\pi = \eta$, force matrix elements in the initial group operator defined basis $|gA\rangle$, $|gB\rangle$, and $|g\sigma_5 B\rangle$, are calculated using Table I. The force matrix blocks in Fig. 12 are formed from these initial matrix elements using icosahedral symmetry projection, and numerically diagonalized using a Householder diagonalization routine. The resulting eigenfrequencies are then plotted to form the trajectories.

A line drawn parallel to the frequency axis in Fig. 13, and positioned along the $\pi = \eta$ axis will intersect a total of 46 trajectories. The points of intersection correspond to the

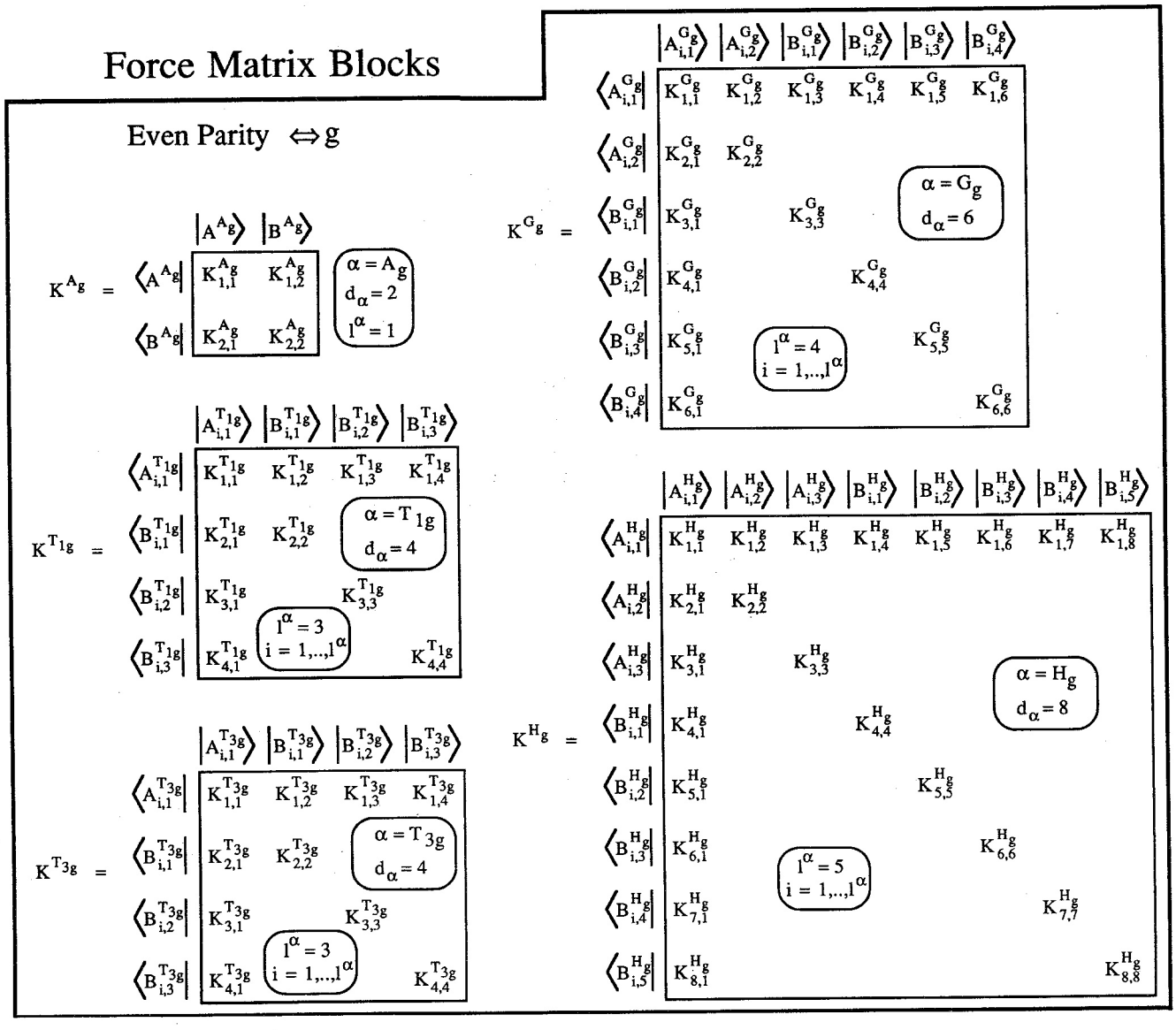

FIG. 12. Block diagonal elements of the force matrix obtained by icosahedral symmetry projection.

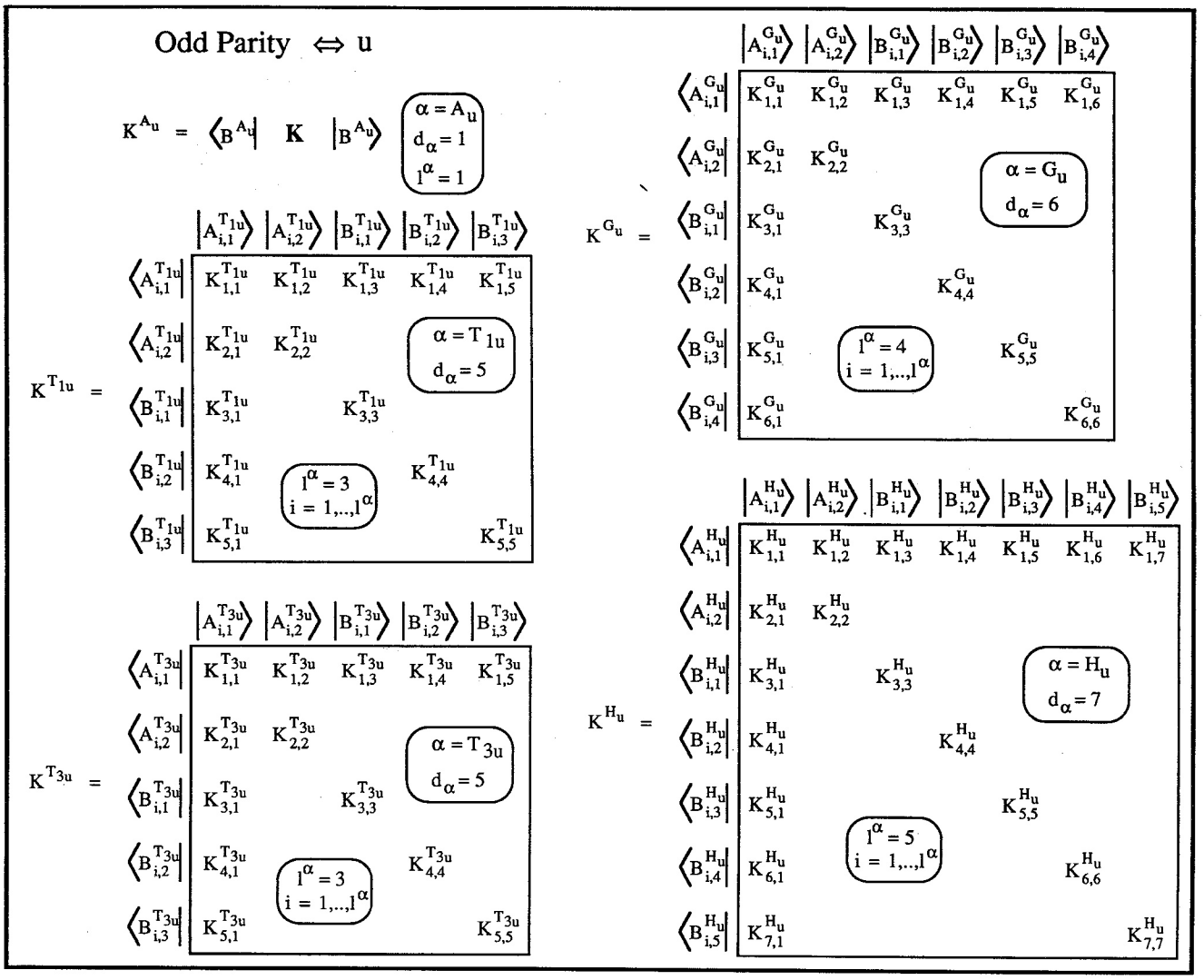

FIG. 12 (*continued*).

vibrational eigenvalues of buckyball for any particular choice of $\pi = \eta$. Only 14 of the 46 distinct eigenvalues will be observable with dipole or Raman spectroscopy. Four of these 14 eigenfrequencies correspond to the three-fold degenerate first-order dipole active T_{1u} modes. The fifth of the $d_{T_{1u}} = 5$ T_{1u} modes corresponds to zero frequency translation in three orthogonal directions. The remaining 10 observable eigenfrequencies correspond to first-order Raman active modes. Eight of these are the $d_{H_g} = 8$ fivefold degenerate H_g modes, and two are the $d_{A_g} = 2$ nondegenerate A_g modes.

The lower bound of any set of buckyball vibrational eigenfrequencies for $p = h = 1$ and $0 \leqslant \pi = \eta \geqslant 1$, is determined by the lowest H_g trajectory. The upper bound is very nearly determined by the highest H_g trajectory. The two A_g trajectories are parallel to the $\pi = \eta$ axis and are therefore independent of the bending spring constants. This will be useful in the comparison of experimental and theoretical spectra because the two stretching spring constants p and h can be determined from the two A_g eigenfrequencies.

By plotting eigenvalue trajectories, a set of physically relevant spring constants is most likely to be used. A reasonable choice of spring constants may be obtained from benzene which is similar to hexagonal fragment of buckyball,[23]

$$h = 7.6\times 10^5 \text{ dyn/cm} = p\,,$$

$$\eta = 0.7\times 10^5 \text{ dyn/cm} = \pi\,. \tag{5.1}$$

The spring constant p has been set equal to h because any actual difference between the two is probably beyond the accuracy of this initial choice. For the same reason π is set equal to η. Using these spring constants, a reasonable prediction of the vibrational buckyball spectrum lies at about $\pi = \eta = 0.1$ in Fig. 13. Nearby at $\pi = \eta = 0.17$ there is a nearly degenerate avoided crossing between the two lowest dipole active T_{1u} trajectories. As a result the lowest two dipole active eigenfrequencies will be closely spaced. A synthetic spectrum of the dipole and Raman active modes using spring constants given in Eq. (5.1) is shown in Fig. 14. A list

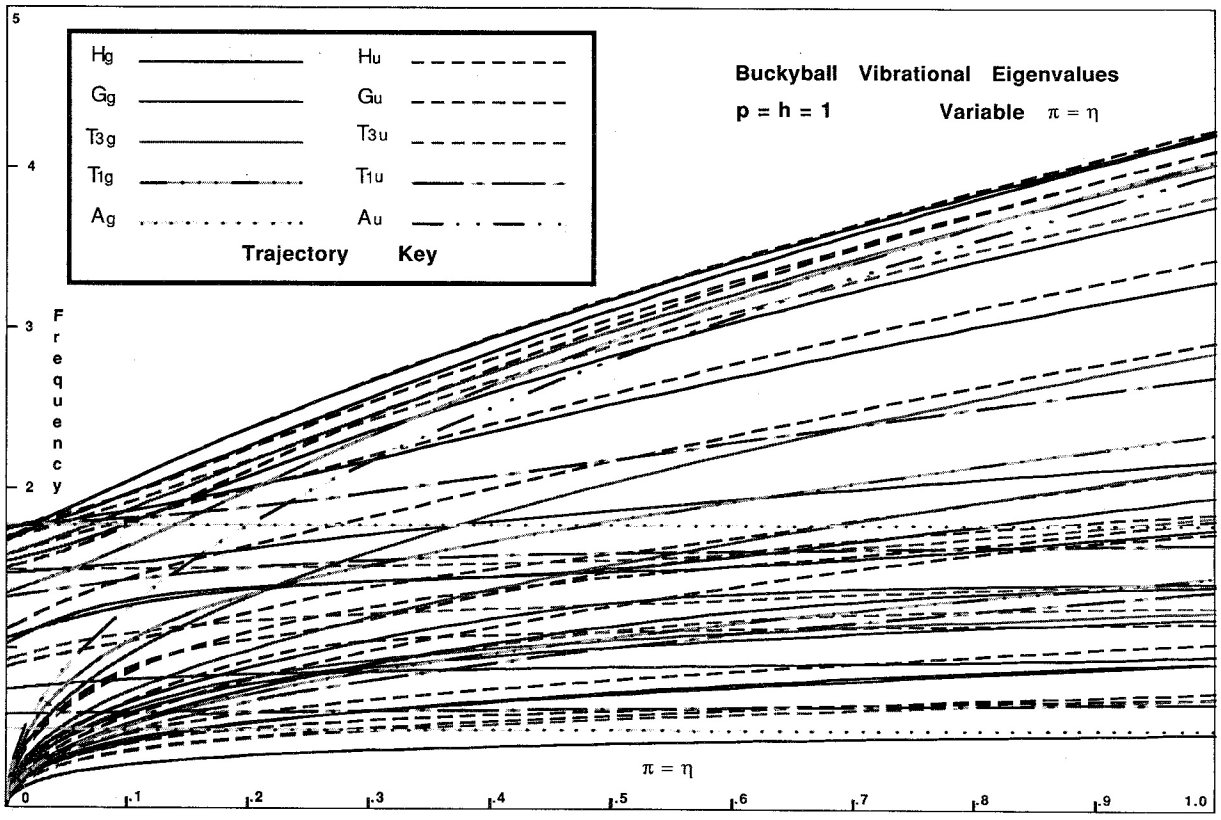

FIG. 13. Buckyball vibrational eigenvalue trajectories. Note the near degenerate avoided crossing of the lowest two T_{1u} trajectories at $\pi = \eta = 0.17$.

of all 46 distinct buckyball vibrational eigenfrequencies using the same spring constants is given in Table III.

The l^α identical force matrix blocks K^α in Fig. 12 are diagonalized by l^α identical transformation matrices T^α. The T^α mix the projection operator bases $|O^\alpha_{ij}\rangle$ to form eigenvectors $|\alpha_{bc}\rangle$,

$$|\alpha_{b,c}\rangle = \sum_i T^\alpha_{i,c} |O^\alpha_{b,i}\rangle \,. \tag{5.2}$$

In Eq. (5.2) the index b runs from 1 to l^α and labels the l^α degenerate partners that correspond to the l^α identical force matrix blocks K^α. The index c runs from 1 to d_α and labels the column of the b th force matrix block to which the eigenvector belongs. The index i of the transformation T^α runs from 1 to d_α, and the corresponding index i of the $|O^\alpha_{b,i}\rangle$ effectively runs from 1 to d_α when both orbit labels A and B are used. Eigenvalues that correspond to the $|\alpha_{bc}\rangle$ are labeled ω^α_c. The initial force matrix was block diagonalized by the transformation Q given by Eq. (4.2). The elements of Q are the overlaps between the original group operator defined basis $|gA\rangle$, $|gB\rangle$, $|g\sigma_5 B\rangle$, and the projection operator basis $|O^\alpha_{i,j}\rangle$. Multiplication of Q and T yields the matrix R that directly diagonalizes the initial force matrix. Elements of the matrix R are overlaps between the original group operator defined basis and the eigenvectors of the force matrix,

$$\sum_{i=1}^{d_\alpha} Q^\alpha_{gO,bi} T^\alpha_{ic} = R^\alpha_{gO,bc} = \sum_{i=1}^{d_\alpha} \langle gO|O^\alpha_{bi}\rangle \langle O^\alpha_{bi}|\alpha_{bc}\rangle$$

$$= \langle gO|\alpha_{bc}\rangle \,. \tag{5.3}$$

These overlaps are coefficients of the eigenvectors of the force matrix in an expansion of the initial group operator defined basis vectors. In general these coefficients may be complex. At time $t=0$ the real parts $\mathrm{Re}\{\langle gA|\alpha_{bc}\rangle\}$, $\mathrm{Re}\{\langle gB|\alpha_{bc}\rangle\}$, and $\mathrm{Re}\{\langle g\sigma_5 B|a_{bc}\rangle\}$ determine the displacement of each of the 60 masses of buckyball located at the vertices labeled g, in the $\overrightarrow{gA}$, $\overrightarrow{gB}$, and $\overrightarrow{g\sigma_5 B}$ directions. The imaginary parts $\mathrm{Im}\{\langle gA|\alpha_{bc}\rangle\}$, $\mathrm{Im}\{\langle gB|\alpha_{bc}\rangle\}$, and $\mathrm{Im}\{\langle g\sigma_5 B|a_{bc}\rangle\}$ determine the momentum of each of the 60 masses in the corresponding directions.

The real and imaginary parts of the coefficient $\langle gO|\alpha_{bc}\rangle$ are also the coordinates of the gOth phasor in the two-dimensional gOth phase space where the real axis corresponds to the displacement of the gth mass in the $\overrightarrow{gO}$ direction, and the imaginary axis corresponds to the scaled momentum $P/m\omega$ of the gth mass. The phase of the gOth phasor is given by

$$\beta_{gO} = \arctan\left\{\frac{\mathrm{Im}(\langle gO|\alpha_{bc}\rangle)}{\mathrm{Re}(\langle gO|\alpha_{bc}\rangle)}\right\},$$

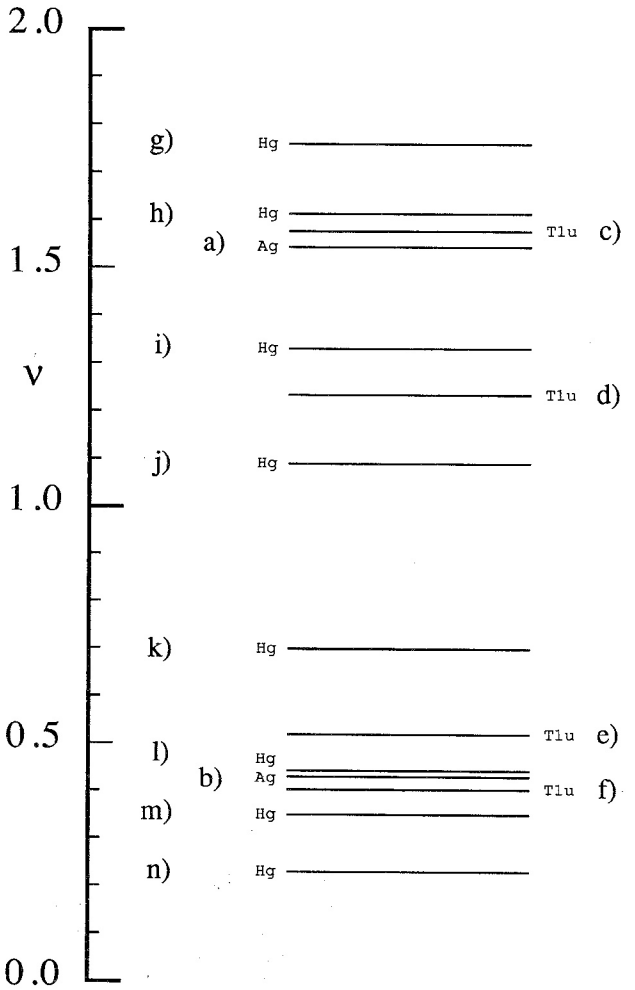

FIG. 14. Synthetic spectrum of the Raman and dipole active modes of buckyball. Spring constants are those of benzene given in Eq. (5.1). The scale is in units of 1185 cm^{-1}. Lines a–n correspond to teh A_g, T_{1u}, and H_g modes in Figs. 15(a)–15(n).

TABLE III. Symmetry labeled eigenfrequencies of buckyball for spring constants of benzene given in Eq. (5.1).

Even parity		Odd parity	
I_h group label	Frequency (1/cm)	I_h group label	Frequency (1/cm)
A_g	1830	A_u	1243
	510		
		T_{1u}	1868
T_{1g}	1662		1462
	1045		618
	513		478
T_{3g}	1900	T_{3u}	1954
	951		1543
	724		1122
	615		526
			358
G_g	2006		
	1813	G_u	2004
	1327		1845
	657		1086
	593		876
	433		663
			360
H_g	2085		
	1910	H_u	2086
	1575		1797
	1292		1464
	828		849
	526		569
	413		470
	274		405

and evolves in time with an angular frequency ω_c^α. When the coefficients in Eq. (5.3) are complex, the β_{gO} phasors will be out of phase and the displaced gth mass will never pass through its equilibrium position. In general, the trajectory of the gth mass will be elliptical and will have some associated vibrational angular momentum. This will couple with any existing rotational angular momentum and split the l^α degeneracies. These complex normal modes are referred to as moving waves because at no time do any of the masses have pure displacement and no momentum. When the coefficients in Eq. (5.3) are pure real, the β_{gO} phasors will be in phase or out of phase by 180°. This means that at $t=0$ all masses are maximally displaced, at $t=\pi/2\omega$ all masses pass through their equilibrium positions, and at $t=\pi/\omega$ all masses reach maximal displacement in the opposite direction. Normal modes that display this degenerate elliptical motion, where the trajectories of all 60 masses are straight lines, are refered to as standing waves.

Stereographic figures of the four dipole and ten Raman active normal modes of buckyball are shown in Fig. 15 and correspond to the 14 spectral lines in Fig. 14. These figures are single snapshots at time $t=0$ of computer generated three-dimensional (3D) movies of normal mode standing waves that were generated by a MacIntosh 512K personal computer. The modes are labeled by icosahedral irreps α, icosahedral subgroup chains, parity, force matrix column number, and partner number. For example, a typical dipole label is given by

*T*1	*D*5*S*	*U*	1	PARTNER No. 1
Icosahedral irrep label	Icosahedral subgroup chain	Parity	Force matrix column	Partner

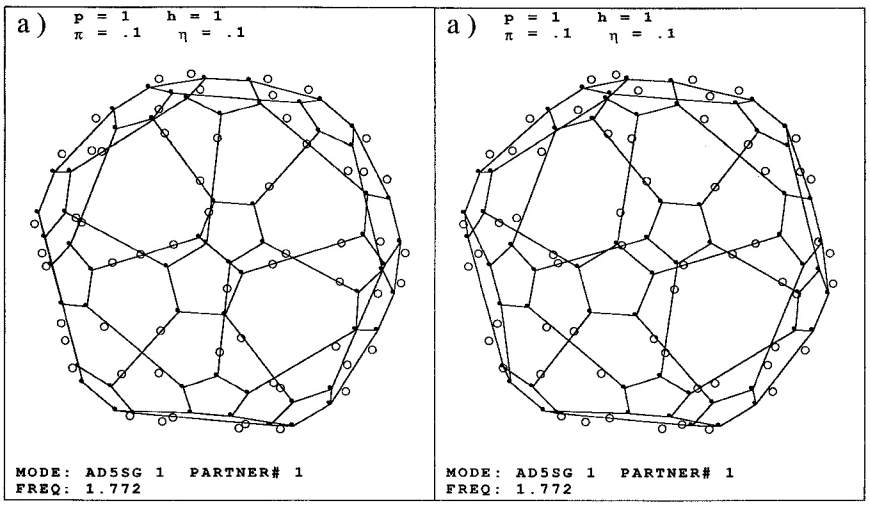

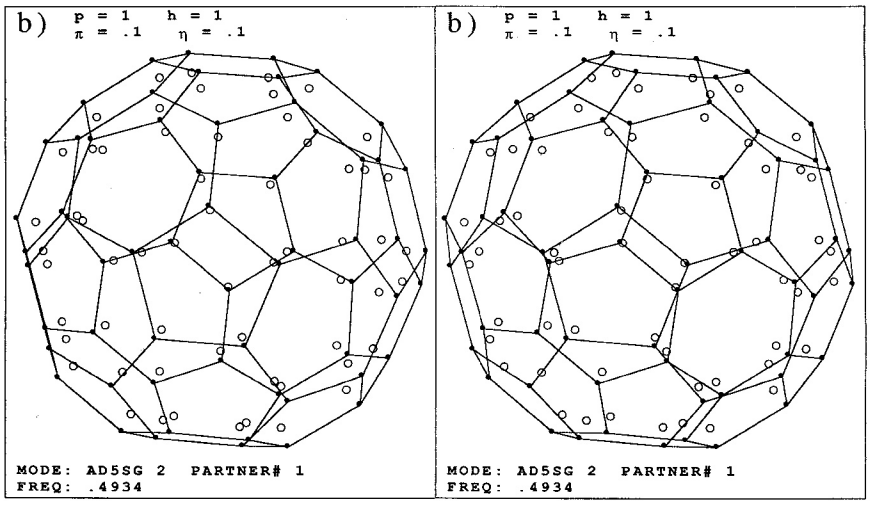

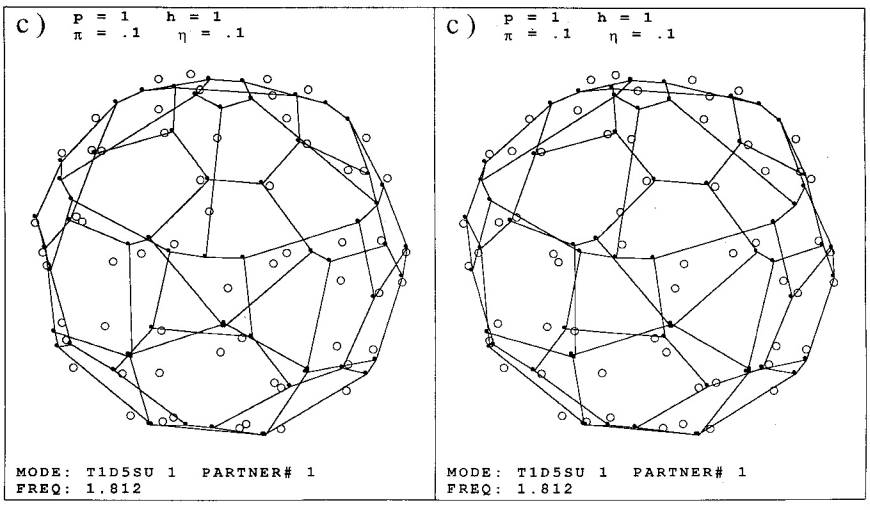

FIG. 15. Stereoscopic views of the (a)–(b) A_g, (c)–(f) T_{1u}, and (g)–(n) H_g modes of buckyball. Stretching and bending spring constants given at the top of each figure have approximately the same ratio as those of benzene given in Eq. (5.1). Mode labels and frequencies in units of 1010 cm^{-1} are given at the bottom of the figures. Modes (a)–(n) correspond to spectral lines a–n in Fig. 14.

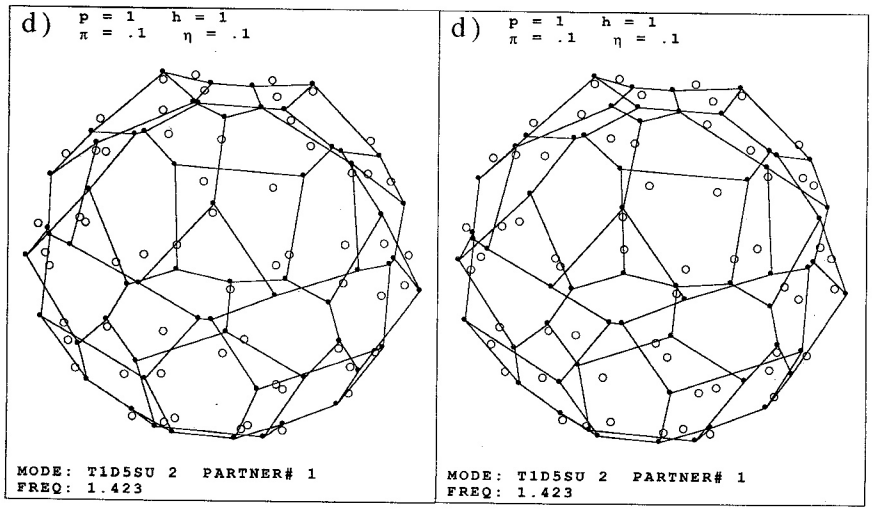

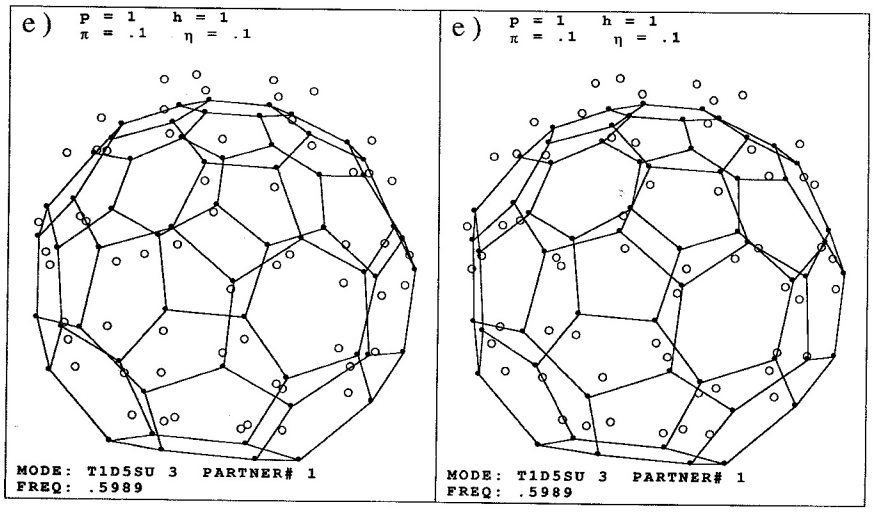

FIG. 15 (*continued*).

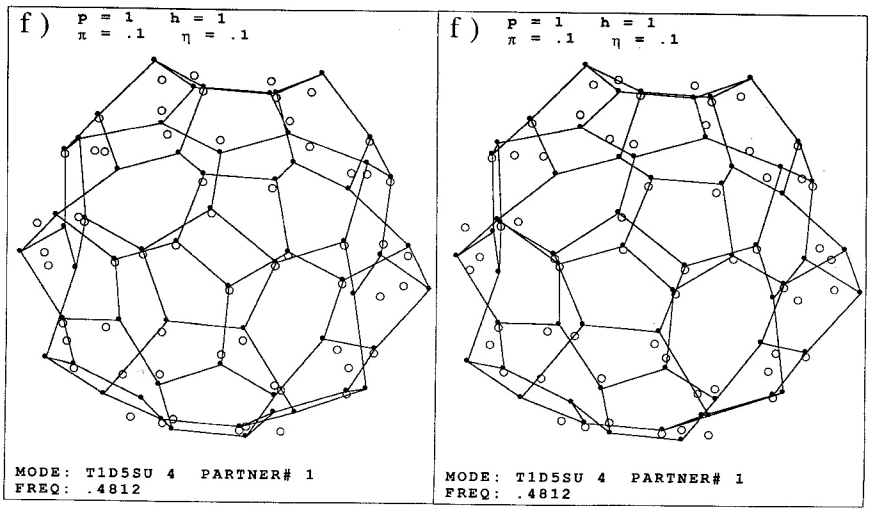

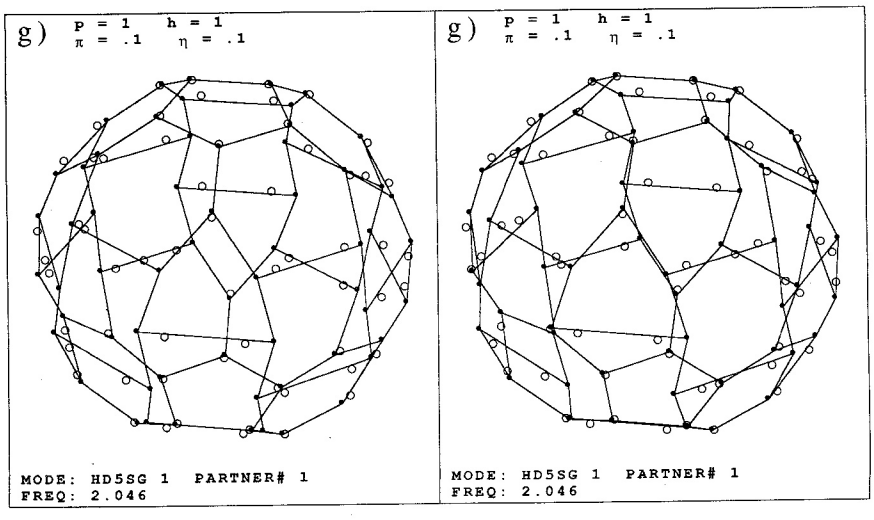

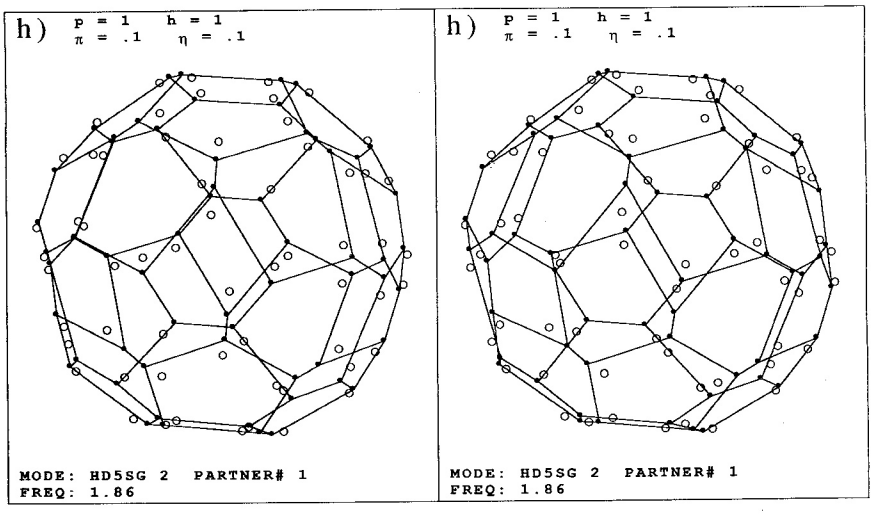

FIG. 15 (*continued*).

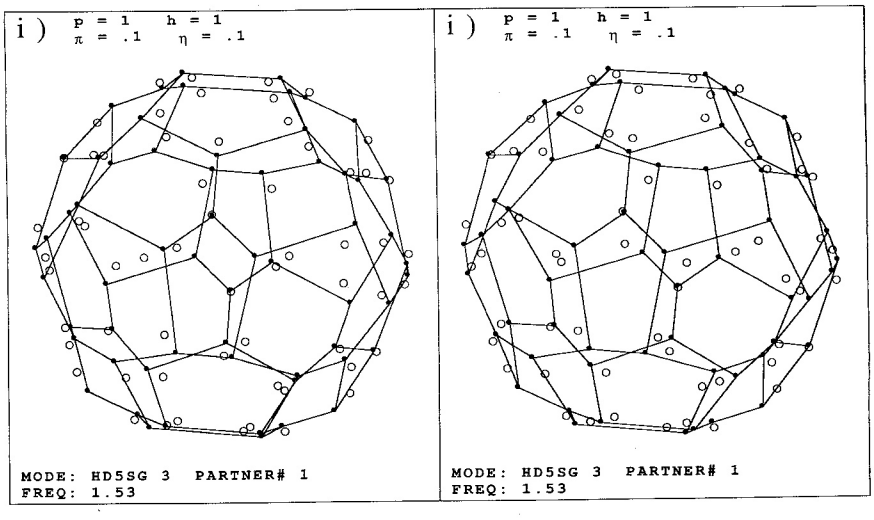

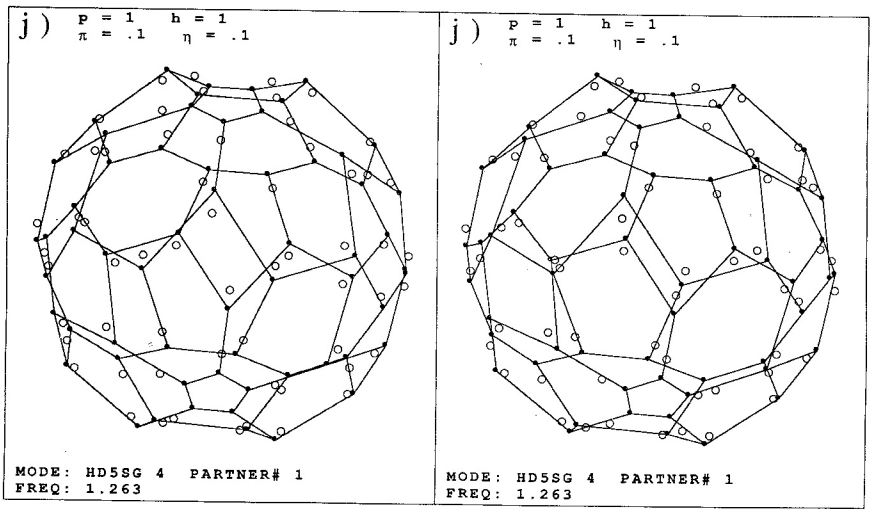

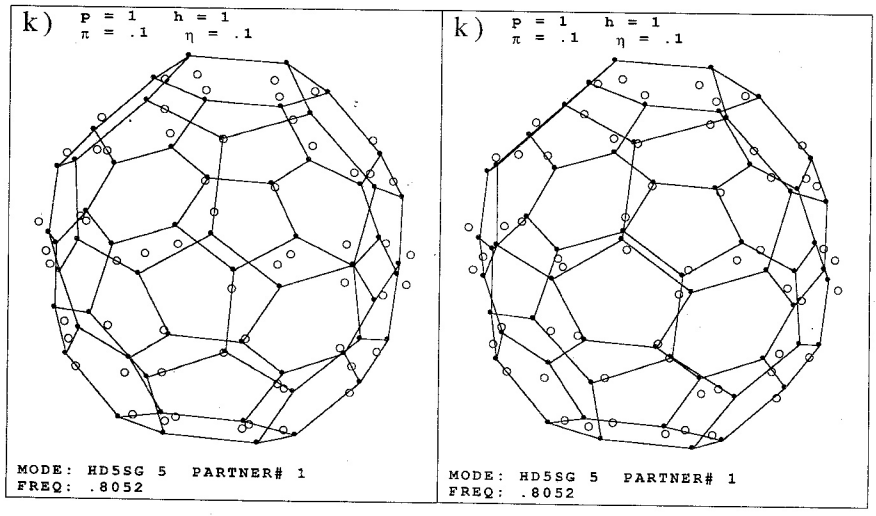

FIG. 15 (*continued*).

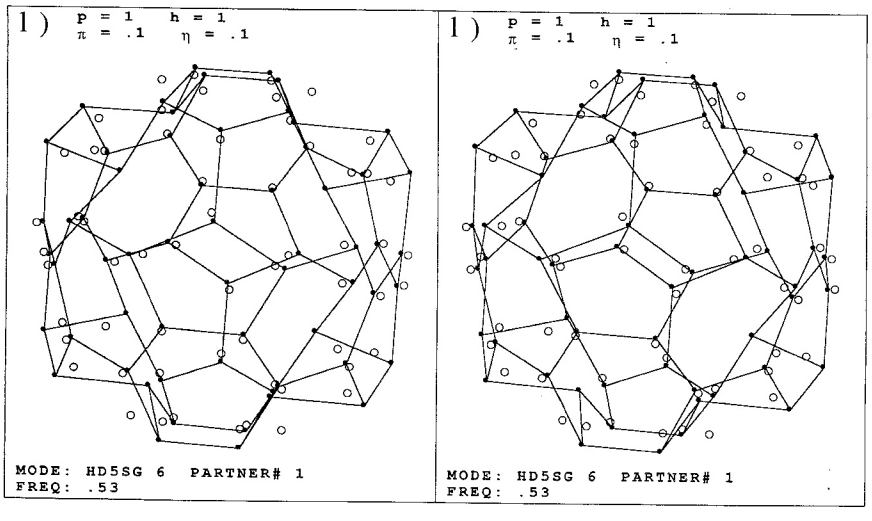

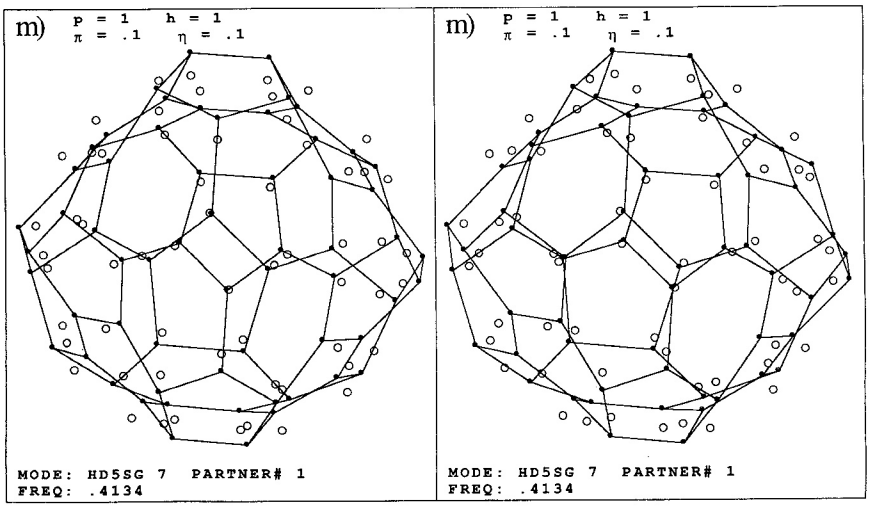

FIG. 15 (*continued*).

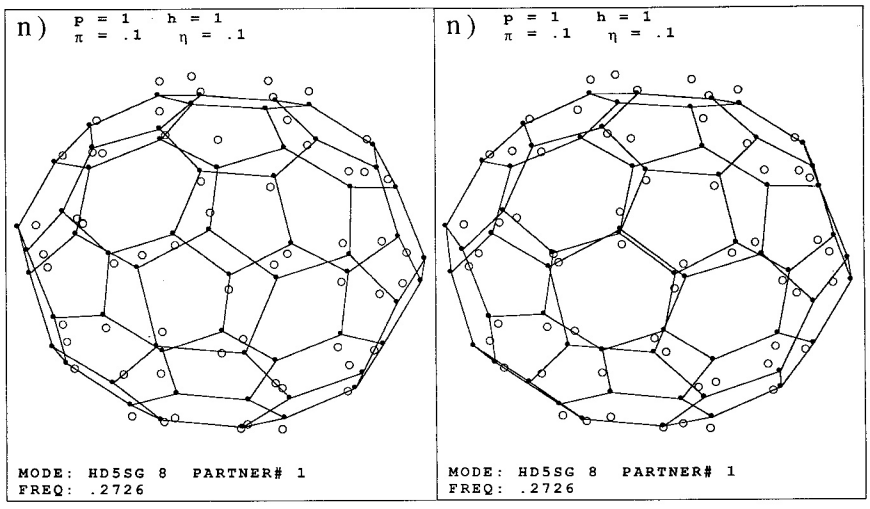

The icosahedral subgroup chain label $D\,5S$ identifies which particular set of equivalent icosahedral irreps were used in Eqs. (4.2) and (5.3) to calculate the normal mode. The partner number distinguishes between the l^{α} degenerate modes.

Only the first partner of the two A_g, four T_{1u}, and eight H_g modes are shown in Fig. 15. The two nondegenerate A_g modes consist of a higher frequency "pentagonal pinch" mode and a lower frequency "breathing" mode. In both A_g modes only the edge lengths change while the vertex angles $\theta(g)$, $\phi(g)$, and $\gamma(g)$ remain constant and equal to their equilibrium values $\Theta(g) = 108°$, $\Phi(g) = 120°$, and $\Phi(g) = 120°$. This is expected because the A_g irrep label indicates that the A_g modes are icosahedrally invariant which is violated if the angles change. This agrees with the earlier conclusion that the A_g eigenvalues are independent of the bending spring constants.

The dipole nature of the T_{1u} modes can be seen in Figs. 15(a)–15(d). In the three highest frequency modes the top pentagon is constricted while the bottom pentagon is distended. This distortion of the nuclei, as they alternately crowd toward the top and then bottom pentagon, shifts charge symmetrically along an axis that passes through the center of the pentagons and defines the dipole axis of the mode. The lowest frequency mode has top and bottom pentagons that remain the same size and move up and down in concert while the remaining nuclei move in the opposite direction in order to satisfy the translational Eckart condition.[24] This also has the effect of creating a dipole moment along the axis passing through both pentagons. The remaining two degenerate partners of the four T_{1u} modes generate dipole moments in orthogonal directions.

In the absence of a central atom and strong radial bonds, the higher frequency normal modes of buckyball correspond

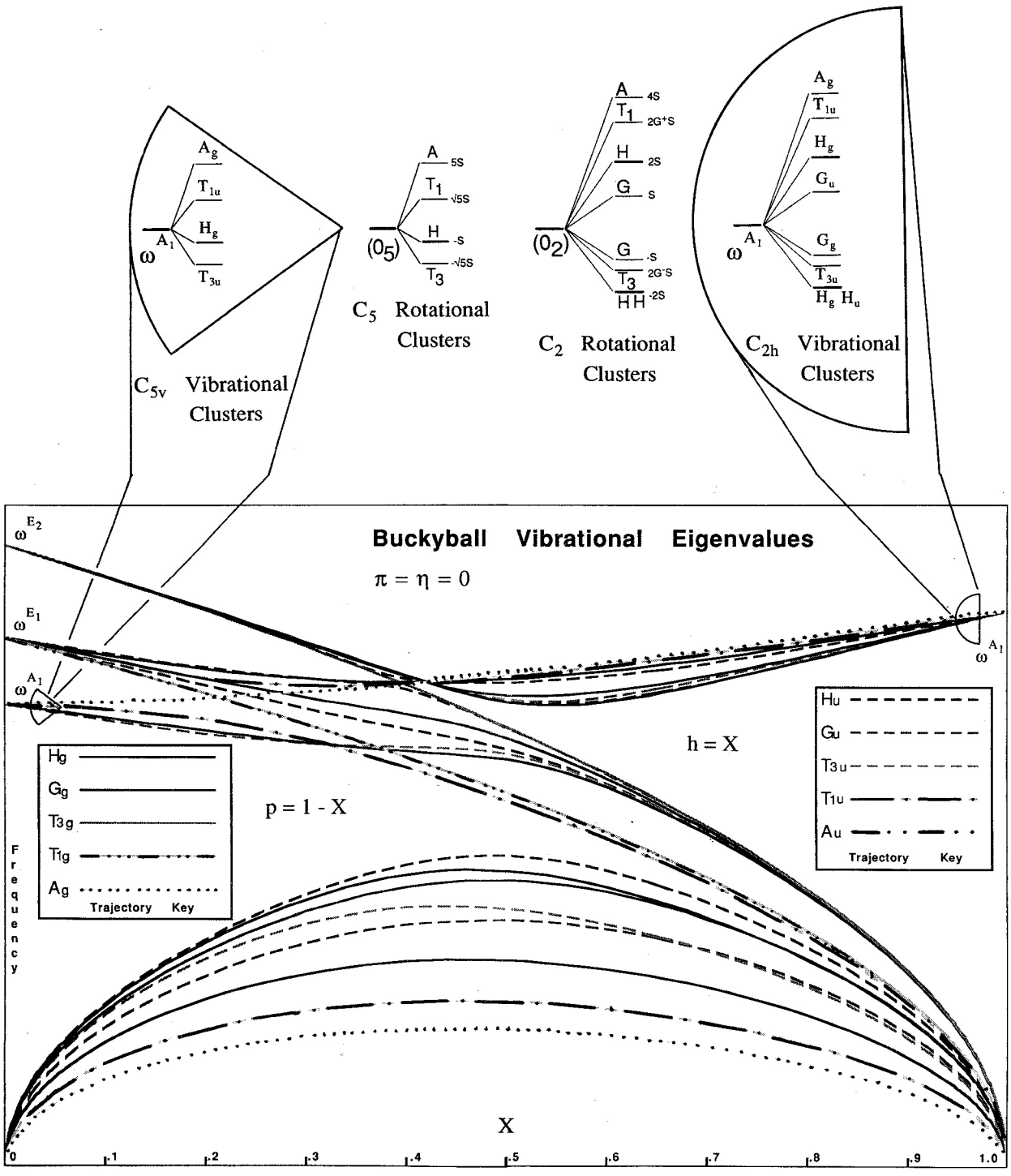

to primarily tangential motion of the carbon atoms. This motion distorts the stretching and bending springs to a greater degree than radial motion. This is why the tangential "pentagonal pinch" A_g mode is higher in frequency than the radial "breathing" A_g mode. A progression from tangential to radial motion can also be observed in the T_{1u} and H_g modes as a function of the frequency of the mode. For example, the highest frequency H_g mode is almost purely tangential while the lowest frequency H_g mode is almost an entirely radial distortion of buckyball into an ellipsoid.

VI. SPECIAL CASES

In Sec. V the behavior of the buckyball spring-mass model was studied with all four spring constants p, h, π, and η assigned nonzero values. With appropriate choices of spring constants set to zero, it is possible to study systems with reduced symmetry for which independent analytic results are available. Comparisons between the analytic results, and those obtained by icosahedral symmetry projection and subsequent numerical diagonalizations, provide a

a) $I_h \downarrow C_{2h}$

	A_1	A_2	B_1	B_2
A_g	1	0	0	0
T_{1g}	0	1	1	1
T_{3g}	0	1	1	1
G_g	1	1	1	1
H_g	2	1	1	1
A_u	0	0	0	1
T_{1u}	1	1	1	0
T_{3u}	1	1	1	0
G_u	1	1	1	1
H_u	1	1	1	2

b) $I_h \downarrow C_{5v}$

	A_1	A_2	E_1	E_2
A_g	1	0	0	0
T_{1g}	0	1	1	0
T_{3g}	0	1	0	1
G_g	0	0	1	1
H_g	1	0	1	1
A_u	0	1	0	0
T_{1u}	1	0	1	0
T_{3u}	1	0	0	1
G_u	0	0	1	1
H_u	0	1	1	1

FIG. 17. The $I_h \supset C_{2h}$ and $I_h \supset C_{5v}$ subgroup correlation tables.

check on the validity of the general computational procedure.

The five choices of spring constants are as follows.

(i) $p \neq 0$, $h \neq 0$, $\pi \neq 0$, $\eta \neq 0$. When all four spring constants are nonzero, six of the $3 \times 60 = 180$ eigenvectors correspond to zero frequency motion. Three of these motions are the $l^{T_{1u}} = 3$, fifth column, T_{1u} translation, and three are the $l^{T_{1g}} = 3$, fourth column, T_{1g} rotations. The I_h irrep label T_{1u} is odd and corresponds to the polar nature of translation, while the irrep label T_{1g} is even and corresponds to the axial nature of rotation.

(ii) $p \neq 0$, $h \neq 0$, $\pi = \eta = 0$. By setting the bending spring constants π and η to zero, 90 of the $3 \times 60 = 180$ eigenvectors of the force matrix will correspond to zero frequency motion. Six of these motions are the T_{1u} translations and T_{1g} rotations. The remaining 84 zero frequency motions correspond to first-order distortions of buckyball that change the vertex angles $\theta(g)$, $\phi(g)$, and $\gamma(g)$ without stretching the edges. A set of eigenvalue trajectories for $\pi = \eta = 0$ is given in Fig. 16 where the stretching spring constants p and h are varied as a function of the parameter X,

$$p \equiv p(X) = 1 - X,$$

$$h \equiv h(X) = X, \quad 0 \leqslant X \leqslant 1. \tag{6.1}$$

(iii) $p = \pi = \eta = 0$, $h = 1$. When $X = 1$ in Eq. (6.1) the pentagonal stretching spring is 0 and the hexagonal stretching spring is 1. This choice of spring constants isolates 30 pairs of masses each aligned with one of the 30 icosahedral edges indicated by the thick lines in Fig. 2. The masses in each pair are coupled by a single hexagonal spring, forming 30 independent C_{2h} symmetric vibrational systems. The only nonzero frequency normal mode of these systems is the symmetric stretch labeled by the C_{2h} irrep A_1. The A_1 column of the $I_h \supset C_{2h}$ correlation table given in Fig. 17(a) determines which buckyball normal modes will simultaneously yield the symmetric stretch motion for each of the 30 vibrational systems. Eigenvalue trajectories in Fig. 16 corresponding to these modes converge to the single C_{2h} symmetric stretch eigenfrequency as $X \to 1$. The analytic solution of the symmetric stretch eigenfrequency is found quite easily to be

$$\omega^{A_1} = \sqrt{2h/m},$$

where for $h = m = 1$, $\omega^{A_1} = \sqrt{2}$. This is the frequency obtained using icosahedral symmetry projection which verifies the general calculational procedure. In particular it tests the geometry used to determine the potential dependence on the hexagonal spring constant h in Eq. (3.3a).

(iv) $h = \pi = \eta = 0, p = 1$. When $X = 0$ in Eq. (6.1) the pentagonal stretching spring constant becomes one and hexagonal spring constant becomes zero. This choice of spring constants isolates 12 sets of five masses. Each mass is located at the vertex of a pentagon and is connected to the other masses of the pentagon with a pentagonal stretching spring. This forms 12 independent C_{5v} symmetric vibrational systems indicated by the thin lines in Fig. 2. Out of ten possible C_{5v} vibrations, one is a zero frequency A_2 rotation, two are zero frequency E_1 translations, and two are E_2 bending motions with zero frequency when $\pi = 0$. The five remaining C_{5v} normal modes consist of an A_1 breathing mode, two degenerate E_1 modes, and two degenerate E_2 modes. The A_1,E_1, and E_2 columns of the $I_h \supset C_{5v}$ correlation table in Fig. 17(b) determine which normal modes of buckyball will yield A_1, E_1, and E_2 type C_{5v} motions in each of the 12 isolated pentagons. Eigenvalue trajectories in Fig. 16 corresponding to these buckyball normal modes converge to the three A_1, E_1, and E_2 type C_{5v} eigenfrequencies as $X \to 0$. These agree with analytic solutions in the independent calculation of the A_1, E_1, and E_2 eigenfrequencies using C_{5v} projection methods given in Appendix A. For $p = m = 1$ these are,

$$\omega^{A_1} = \{\tfrac{1}{2}(5 - \sqrt{5})\}^{1/2} = 1.715\,570\,505\ldots,$$

$$\omega^{E_1} = \left\{1 + \cos\left(\frac{\pi}{5}\right)\right\}^{1/2} = 1.344\,997\,024\ldots,$$

$$\omega^{E_2} = \{\tfrac{5}{2}\}^{1/2} = 1.581\,138\,83\ldots.$$

This provides a further test of the general computational procedure and indicates that the potential dependence on the pentagonal springs p is treated correctly.

(v) $p = h = \eta = 0$, $\pi = 1$. The C_{5v} symmetry described in (iv) is unchanged with this choice of spring constants. There are two nonzero C_{5v} eigenvalues that correspond to doubly degenerate E_1 modes and doubly degenerate E_2 bending modes. The A_1 breathing mode is independent of bending and is a zero frequency distortion in the absence of the pentagonal stretching spring. Analytic values calculated in Appendix A for $\pi = m = 1$ are,

$$\omega^{E1} = \{\tfrac{5}{2}\}^{1/2} = 1.581\,138\,83\ldots,$$

$$\omega^{E2} = \frac{\sqrt{5}}{2}\{5 + \sqrt{5}\}^{1/2} = 3.007\,504\,78\ldots.$$

These values are also obtained using the general computational procedure and verify that the more complicated po-

tential dependance on the pentagonal spring constant π, in Eq. (3.3b), is correct.

A direct test of the hexagonal bending spring η is difficult because this spring couples all 60 masses in the buckyball model. However, the symmetric nature of the force matrix blocks in Fig. 12, the independence of vibrational eigenvalues with respect to the choice of equivalent sets of icosahedral irreps used in Eq. (4.2), and the observed bending spring independence of the A_g modes, all serve as indirect evidence that the potential dependance on the hexagonal spring η is also correct.

The buckyball eigenvectors determined by the A_1 column of the $I_h \supset C_{2h}$ correlation table span the 30-dimensional C_{2h}-induced-to-I_h repesentation. In this basis a force matrix is diagonal when $p = \pi = \eta = 0$ and $h = 1$. With this choice of spring constants all 30 diagonal elements are equal to the C_{2h} symmetric stretch eigenfrequency. By weakly coupling the 30 C_{2h} symmetric vibrational systems with the pentagonal stretching spring, the 30-fold degeneracy is split into eight clustered levels shown in the upper right-hand side of Fig. 16. This splitting is the classical analogue of the 0_2 type C_2-induced-to-I rotational superfine cluster also shown in the upper right-hand side of Fig. 16.[13,14] Calculation of the cluster splittings in both cases involves the construction of a coset space and the definition of an appropriate initial state vector $|1A\rangle$. In the case of the rotational superfine splitting this initial state vector represents a wave packet with 0_2-type C_2 local symmetry localized on one of the 30 icosahedral edges, and is the probability amplitude for finding the angular momentum vector in a set of body-fixed coordinates. The C_2 coset space is spanned by state vectors generated from the initial state vector using C_2 coset leaders. In this basis the rotational Hamiltonian couples the state vectors with a parameter S that determines the nearest-neighbor tunneling rate between twofold symmetric minima of the icosahedral rotational energy surface. The rotational superfine splitting is obtained by diagonalizing the rotational Hamiltonian using icosahedral symmetry projection. In the classical analogue, the initial state vector is a pair of C_{2h} symmetrically stretched masses located along one of the 30 edges of the icosahedron. This state is spread to the other icosahedral edges with the coset leaders of C_{2h} in I_h. In this basis a force constant operator couples nearest-neighbor states. The coupling is parametrized by the pentagonal stretching spring constant p which is analogous to the rotational tunneling parameter S. Diagonalization of the force matrix yields very

$C_{5v} = \{\ 1 \quad R_1 \quad R_1^2 \quad R_1^3 \quad R_1^4 \quad \sigma_5 \quad \sigma_{10} \quad \sigma_{15} \quad \sigma_8 \quad \sigma_4\ \}$

$D^{A_1}(g) =$	1	1	1	1	1	1	1	1	1	1
$D^{A_2}(g) =$	1	1	1	1	1	-1	-1	-1	-1	-1
$D^{E_1}(g) =$	1 0 0 1	ε −β β ε	γ −τ τ γ	γ τ −τ γ	ε β −β ε	1 0 0 -1	ε β β −ε	γ τ τ −γ	γ −τ −τ −γ	ε −β −β −ε
$D^{E_2}(g) =$	1 0 0 1	γ −τ τ γ	ε β −β ε	ε −β β ε	γ τ −τ γ	1 0 0 -1	γ τ τ −γ	ε −β −β −ε	ε β β −ε	γ −τ −τ −γ
$D^{A_1}(g) =$	1	1	1	1	1	1	1	1	1	1
$D^{A_2}(g) =$	1	1	1	1	1	-1	-1	-1	-1	-1
$D^{E_1}(g) =$	1 0 0 1	α 0 0 α*	δ 0 0 δ*	δ* 0 0 δ	α* 0 0 α	0 1 1 0	0 α α* 0	0 δ δ* 0	0 δ* δ 0	0 α* α 0
$D^{E_2}(g) =$	1 0 0 1	δ 0 0 δ*	α* 0 0 α	α 0 0 α*	δ* 0 0 δ	0 1 1 0	0 δ δ* 0	0 α* α 0	0 α α* 0	0 δ* δ 0

$$\alpha = \exp\left\{2\pi i/5\right\} \qquad \varepsilon = \cos\left\{2\pi/5\right\} = -G^-/2 \qquad \gamma = \cos\left\{4\pi/5\right\} = -G^+/2$$

$$\delta = \exp\left\{4\pi i/5\right\}$$

$$G^{\pm} = \frac{1 \pm \sqrt{5}}{2} \qquad \beta = \sin\left\{2\pi/5\right\} = \left\{\frac{2+G^+}{4}\right\}^{\frac{1}{2}} \qquad \tau = \sin\left\{4\pi/5\right\} = \left\{\frac{3-G^+}{4}\right\}^{\frac{1}{2}}$$

FIG. 18. Two equivalent sets of C_{5v} irreps. Real irreps are given in the first four rows and complex irreps are given in the last four rows.

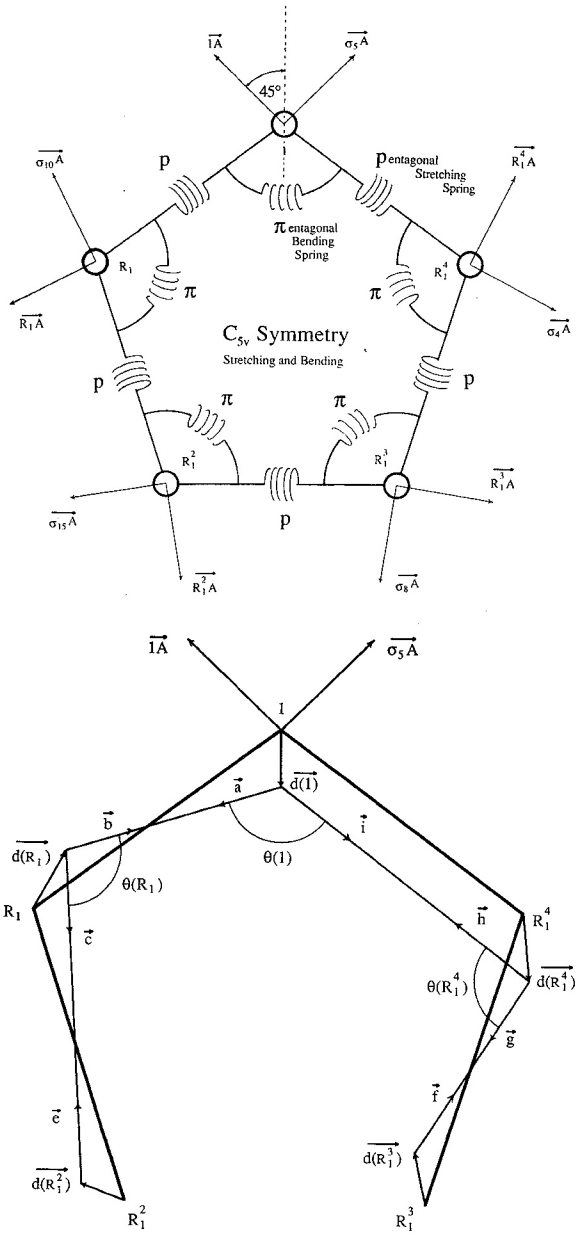

FIG. 19. (a) A C_{5v} symmetric spring-mass model with stretching and bending springs. (b) The unit cell of C_{5v} symmetric spring-mass model. Displacement vectors $\vec{d(g)}$, edge vectors, $\vec{a}$, $\vec{b}$,...,$\vec{l}$, and angles $\theta(g)$ used in the calculation of the potential are labeled.

nearly the same splittings as those in the superfine rotational pattern. Note how long the C_{2h} vibrational cluster pattern is maintained as X decreases. More or less the same pattern persists as X varies from 1 to 0.43 where the cluster forms again to the right of the eightfold trajectory crossing. On the other side of this crossing the pattern quickly disintegrates. A similar comparison is made between the A_1-type C_{5v} vibrational splittings and the 0_5-type C_5 rotational superfine splittings in the upper left of Fig. 16. In this case the hexagonal stretching spring constant h is analogous to the rotational tunneling parameter S, and weakly couples the C_{5v} symmetric pentagonal vibrational systems described in (iv). The C_{5v} clusters centered around ω^{E_1} and ω^{E_2} correspond to E_1 and E_2-type C_{5v}-induced-to-I_h representations of the force constant operator.

TABLE IV. (a) Displacement vectors $d(g)$ used in the calculation of the edge vectors. (b) Edge vectors used to calculate angles.

(a)

$\vec{\mathbf{a}} = \hat{\mathbf{a}} - \mathrm{d}(1) + \mathrm{d}(\mathrm{R}_1)$
$\vec{\mathbf{b}} = \hat{\mathbf{b}} - \mathrm{d}(\mathrm{R}_1) + \mathrm{d}(1)$
$\vec{\mathbf{c}} = \hat{\mathbf{c}} - \mathrm{d}(\mathrm{R}_1) + \mathrm{d}(\mathrm{R}_1^2)$
$\vec{\mathbf{e}} = \hat{\mathbf{e}} - \mathrm{d}(\mathrm{R}_1^2) + \mathrm{d}(\mathrm{R}_1)$
$\vec{\mathbf{f}} = \hat{\mathbf{f}} - \mathrm{d}(\mathrm{R}_1^3) + \mathrm{d}(\mathrm{R}_1^4)$
$\vec{\mathbf{g}} = \hat{\mathbf{g}} - \mathrm{d}(\mathrm{R}_1^4) + \mathrm{d}(\mathrm{R}_1^3)$
$\vec{\mathbf{h}} = \hat{\mathbf{h}} - \mathrm{d}(\mathrm{R}_1^4) + \mathrm{d}(1)$
$\vec{\mathbf{i}} = \hat{\mathbf{i}} - \mathrm{d}(1) + \mathrm{d}(\mathrm{R}_1^4)$

(b)

$$\theta(1) = \arccos\left\{\frac{\vec{\mathbf{a}}\cdot\vec{\mathbf{i}}}{|\vec{\mathbf{a}}||\vec{\mathbf{i}}|}\right\}$$

$$\theta(R_1) = \arccos\left\{\frac{\vec{\mathbf{b}}\cdot\vec{\mathbf{c}}}{|\vec{\mathbf{b}}||\vec{\mathbf{c}}|}\right\}$$

$$\theta(R_1^4) = \arccos\left\{\frac{\vec{\mathbf{g}}\cdot\vec{\mathbf{h}}}{|\vec{\mathbf{g}}||\vec{\mathbf{h}}|}\right\}$$

VII. CONCLUSION

Icosahedral symmetry projection methods applied to the spring-mass model of buckyball provide rapid, testable calculation of rovibronic eigenvalues and eigenvectors. These calculations can be done quickly on a small personal computer such as a MacIntosh 512K. In a few seconds of run time stereographic computer animated movies of vibrational eigenvectors can be generated for any choice of force constants. These eigenvectors are classified by subgroup chain and provide an optimal basis set when considering perturbations such as isotopic variation and corriolis coupling be-

TABLE V. C_{5v} force matrix elements as a function of stretching and bending. Results of numerical and analytical calculations are given where $\theta = 81°$ and $\phi = 9°$.

Force matrix elements	Numerical results: stretching + bending	Analytic results: stretching + bending
$\langle 1A\|F\|1A\rangle$	$= 1.000\,0000p + 2.309\,0170\pi$	$= p + (2 - G^-/2)\pi$
$\langle 1A\|F\|R_1A\rangle$	$= -0.154\,5085p - 1.309\,0170\pi$	$= pG^-/4 + (G^-/2 - 1)\pi$
$\langle 1A\|F\|R_1^2A\rangle$	$= 0.000\,0000p + 0.154\,5085\pi$	$= 0p - \pi G^-/4$
$\langle 1A\|F\|R_1^3A\rangle$	$= 0.000\,0000p + 0.154\,5085\pi$	$= 0p - \pi G^-/4$
$\langle 1A\|F\|R_1^4A\rangle$	$= -0.154\,5085p - 1.309\,0170\pi$	$= pG^-/4 + (G^-/2 - 1)\pi$
$\langle 1A\|F\|\sigma_5A\rangle$	$= -0.309\,0170p + 1.618\,03440\pi$	$= pG^-/2 + \pi G^+$
$\langle 1A\|F\|\sigma_{10}A\rangle$	$= 0.024\,4717p - 2.260\,0735\pi$	$= p\cos^2\theta + (\sqrt{2}\cos\phi/G^-)\pi$
$\langle 1A\|F\|\sigma_{15}A\rangle$	$= 0.000\,0000p + 0.975\,5283\pi$	$= 0p + \pi\cos^2\phi$
$\langle 1A\|F\|\sigma_8A\rangle$	$= 0.000\,0000p + 0.024\,4717\pi$	$= 0p + \pi\cos^2\theta$
$\langle 1A\|F\|\sigma_4A\rangle$	$= 0.975\,5283p - 0.357\,9604\pi$	$= p\cos^2\phi + (\sqrt{2}\cos\theta/G^-)\pi$

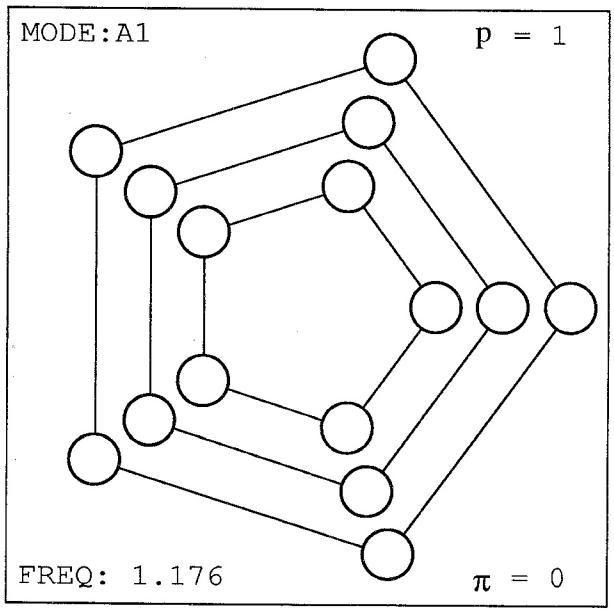

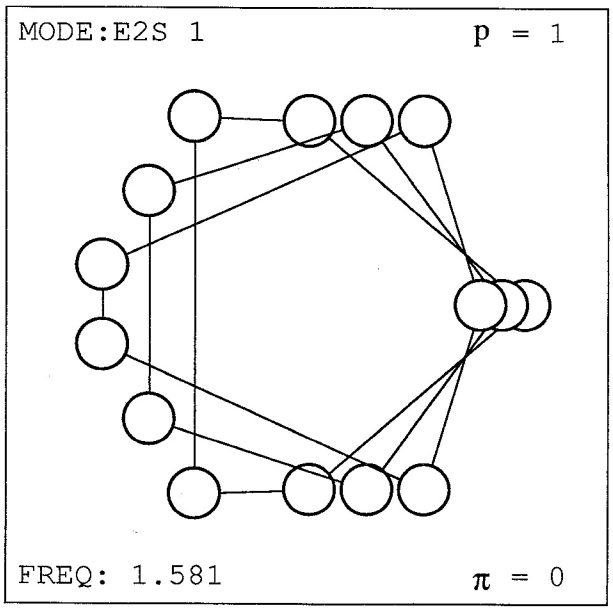

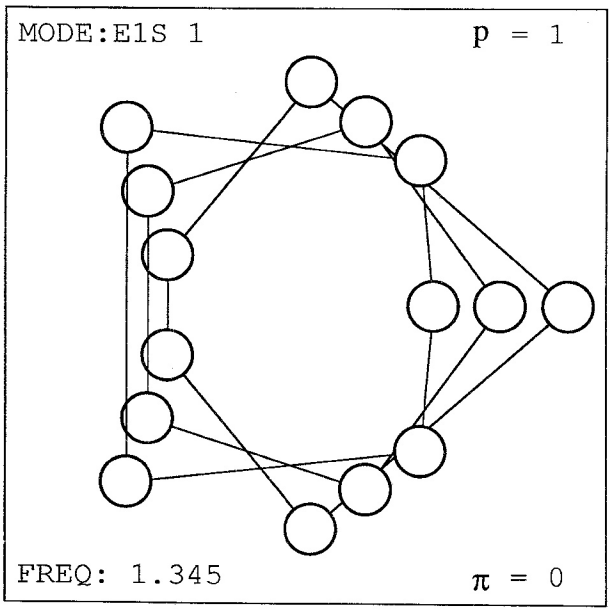

FIG. 20. Normal modes of the C_{5v} symmetric spring-mass model defined by the C_{5v},C_v subgroup chain. Each mode varies as $\cos(\omega t)$ and is plotted at time $t=0$, $t=\pi/2\omega$, and $t=\pi/\omega$. (a) The A_1 "breathing" mode, (b) One of two nonzero frequency vector E_1 modes, and (c) One of two nonzero frequency E_2 modes.

tween rotations and vibrations. This will be useful in the high resolution spectroscopy of buckyball, and will be discussed in future works.

Buckyball animation software for the Macintosh Plus SE, and II that features menus, windows, and button controls is now available. For more information contact D. E. Weeks at the University of Arkansas.

ACKNOWLEDGMENTS

We would like to thank T-12 division at Los Alamos National Laboratory for the use of their facilities. In addition one of us (D. E. W.) would like to thank W. G. Harter for his extensive help without which this work would have been impossible. This research was supported in part by National Science Foundation Grant No. PHY-8696052 in theoretical physics and in part by the Department of the Army.

APPENDIX A: C_{5v} EIGENVALUES AND NORMAL MODES

The icosahedral subgroup C_{5v} contains ten elements consisting of the unit operator, four rotations, and five reflections,

$$C_{5v}=\{1,R_1,R_1^2,R_1^3,R_1^4,\sigma_4,\sigma_5,\sigma_8,\sigma_{10},\sigma_{15}\}\,.$$

A set of C_{5v} irreps is given in Fig. 18.

A spring mass model with C_{5v} symmetry is shown in Fig. 19(a) and is identical to any one of the 12 isolated pentagons described in (iv) and (v) of Sec. VI. The pentagonal stretching and bending spring constants are labeled p and π,

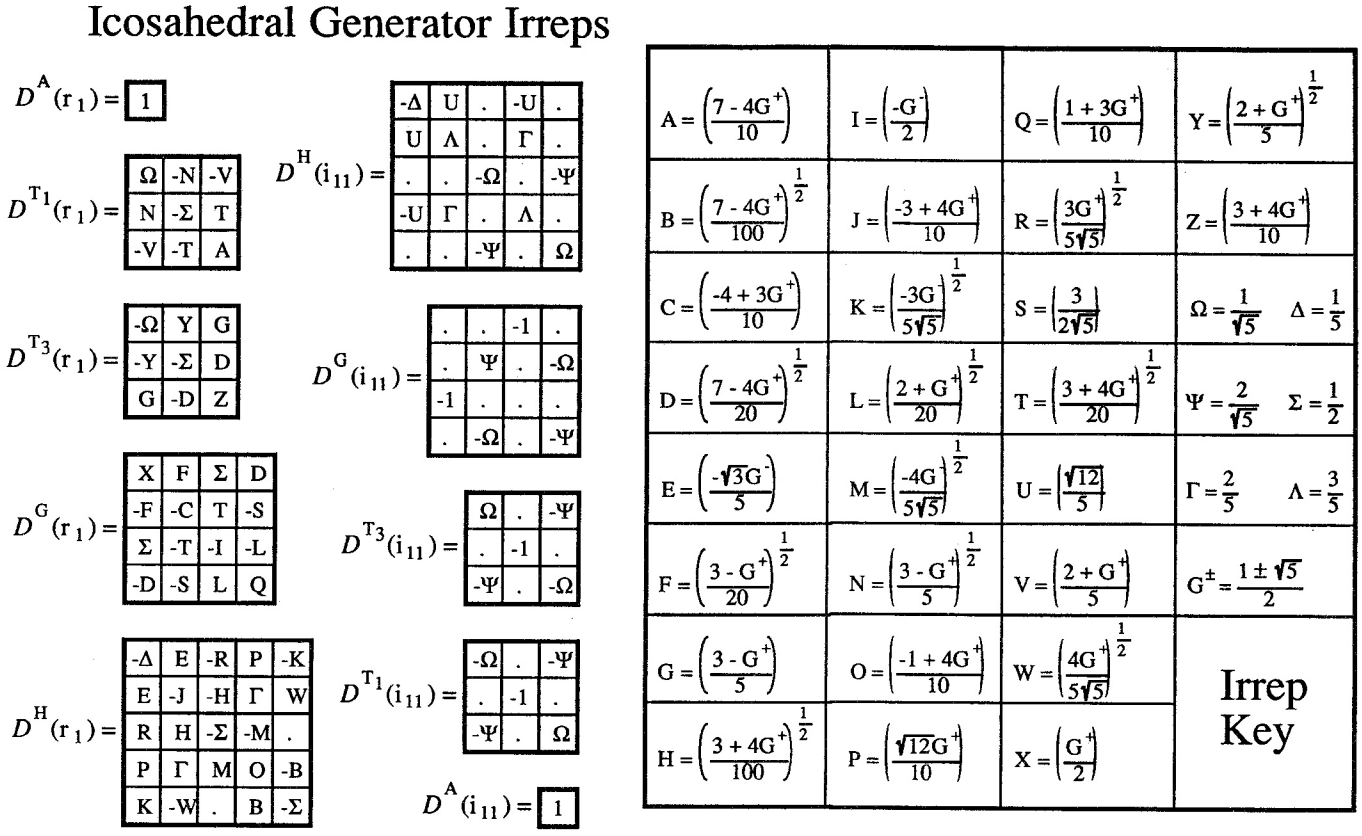

FIG. 21. Icosahedral generator irreps. Rational root form of the irrep elements is given in the irrep key. Irreps of i_{11} are symmetric because the $\omega_i = 180°$ rotations are their own inverses. Rows of the vector irrep T_1 correspond to the z,x, and y body fixed axes shown in Fig. 6.

respectively. All ten springs are contained in the pentagonal plane which permits the problem to be solved using two-dimensional orthogonal coordinate systems located at each mass. These coordinate systems are generated with the $I^{E_1}=2$ dimensional C_{5v} vector irreps $D^{E_1}(g)$, and an initial vector $\overrightarrow{1A}$ rotated 45° away from a radial vector passing through an arbitrary mass. Using the $D^{E_1}(g)$ as rotations in R^2 the initial vector is passed from vertex to vertex generating ten vectors $\overrightarrow{gA}$ that form an orbit labeled A,

$$D^{E_1}(g)\overrightarrow{1A}=\overrightarrow{gA}\,.$$

The C_{5v} group operator labeled vectors $\overrightarrow{gA}$ and of the A orbit are shown in Fig 19(a).

A force constant operator $\mathbf{K}$ is represented in the basis defined by the state vectors $|gA\rangle$ that correspond to the $\overrightarrow{gA}$. Matrix elements of $\mathbf{K}$ in this basis are the second-order derivatives of the potential energy of the unit cell shown in Fig. 19(b). This potential is given by

$$V_s=\frac{p}{2}\{(1-|\vec{\mathbf{a}}|)^2+(1-|\vec{\mathbf{i}}|)^2\}\,,$$
$$V_b=\{[\theta_0-\theta(1)]^2+[\theta_0-\theta(R_1)]^2+[\theta_0-\theta(R_1^4)]^2\}\,, \qquad \text{(A1)}$$
$$V=V_s+V_b\,,$$

where $\theta_0=108°$. The vectors $\vec{\mathbf{a}}$, $\vec{\mathbf{b}}$, $\vec{\mathbf{c}}$,...,$\vec{\mathbf{i}}$, are determined by the displacement vectors $\overrightarrow{d(g)}$ shown in Fig. 19(b), and are listed in (a) of Table IV. Expressions for the angles $\theta(g)$ are given in (b) of Table IV.

The potential in Eq. (A1) is a function of the ten generalized coordinates $x(g)$ and $y(g)$. These are components of the $\overrightarrow{d(g)}$ in a two-dimensional lab-fixed coordinate system. The transformation from $x(g)$, $y(g)$ to the C_{5v} group operator defined set of generalized coordinates gA is made with the C_{5v} E_1 vector irreps. Elements of the force matrix are

	C_1	C_R	C_R^2	C_r	C_i	C_f	C_ρ	C_ρ^2	C_η	C_σ
A_g	1	1	1	1	1	1	1	1	1	1
T_{1g}	3	G^+	G^-	0	-1	3	G^+	G^-	0	-1
T_{3g}	3	G^-	G^+	0	-1	3	G^-	G^+	0	-1
G_g	4	-1	-1	1	0	4	-1	-1	1	0
H_g	5	0	0	-1	1	5	0	0	-1	1
A_u	1	1	1	1	1	-1	-1	-1	-1	-1
T_{1u}	3	G^+	G^-	0	-1	-3	$-G^+$	$-G^-$	0	1
T_{3u}	3	G^-	G^+	0	-1	-3	$-G^-$	$-G^+$	0	1
G_u	4	-1	-1	1	0	-4	1	1	-1	0
H_u	5	0	0	-1	1	-5	0	0	1	-1

$$G^{\pm}=\frac{1\pm\sqrt{5}}{2}$$

FIG. 22. Characters of the full icosahedral group I_h. Characters of the rotation group I are given in the highlighted box.

the second-order derivatives of the potential with respect to the group operator defined coordinates,

$$\langle g'A\,|\mathbf{K}|g''A\rangle = \left|\frac{\partial^2 V(gA)}{\partial g'A\partial g''A}\right|_{\text{equilibrium}}.$$

A four-point central difference method was used to numerically calculate the second-order derivatives. The force matrix elements may also be determined analytically using the geometry of the C_{5v} vibrational system. Stretching spring contributions to matrix elements are determined by the projection of displacements and resulting forces along the pentagonal edges, while bending spring contributions are determined by projecting perpendicular to the edges. Numerical and analytic results are given in Table V and agree for all matrix elements. This verifies the numerical differentiation routine.

The C_{5v} irreps in Fig. 18 and the first row of the force matrix in Table V are used in Eq. (C7) to calculate the block diagonal elements of the force matrix in the C_{5v} irreducible representation. The largest block is 2×2 and is analytically diagonalized using the quadratic formula. The resulting C_{5v} eigenvalues are

$$\omega^{A_1} = \left\{\left(\frac{5-\sqrt{5}}{2}\right)p\right\}^{1/2},$$

$$\omega^{E_1} = \{(1+\cos 36°)p + (\tfrac{5}{2})\pi\}^{1/2}, \tag{A2}$$

$$\omega^{E_2} = \left\{(\tfrac{5}{2})p + \frac{\sqrt{5}}{2}(5+\sqrt{5})\pi\right\}^{1/2}.$$

These results agree with the icosahedral projection results given in Sec. VI. The results given in Ref. 16 for C_{5v} eigenvalues are in serious disagreement with the analytic results in Eq. (A2) which invalidates their predictions for buckyball eigenfrequencies. Normal modes of the C_{5v} spring-mass model are shown in Fig. 20.

APPENDIX B: ICOSAHEDRAL IRREPS

The $\alpha = A$, T_1, T_3, G, and H irreps of the icosahedral rotation group generators r_1 and i_{11} are given in Fig. 21. The remaining irreps of I are generated using the icosahedral multiplication table in Fig. 5. Irreps of the full icosahedral group I_h may be obtained from those of the rotation group I using

I_h irreps I irreps I_h irreps I irreps

$$D^{\alpha_g}(g) = D^{\alpha}(g) \quad D^{\alpha_g}(Ig) = D^{\alpha}(g),$$

$$D^{\alpha_u}(g) = D^{\alpha}(g) \quad D^{\alpha_u}(Ig) = -D^{\alpha}(g).$$

Icosahedral characters are given in Fig. 22.

APPENDIX C: PROJECTION OPERATORS

Projection operators defined in Eq. (4.1) obey simple multiplication rules,

$$P^{\alpha}_{ij}P^{\beta}_{kl} = P^{\alpha}_{il}\delta^{\alpha\beta}\delta_{jk}. \tag{C1}$$

When $i=j$ projection operators are idempotent and hermetian. For $i\neq j$ projection operators are nilpotent,

$$P^{\alpha}_{ii}P^{\alpha}_{ii} = P^{\alpha}_{ii},$$

$$P^{\alpha}_{ij}P^{\alpha}_{ij} = 0,$$

$$P^{\alpha}_{ij} = \{P^{\alpha}_{ji}\}^{\dagger}. \tag{C2}$$

In Eq. (4.1) the indices i and j run from 1 to l^{α}, resulting in $(l^{\alpha})^2$ projection operators P^{α}_{ij} for each irrep α. This means that there are as many projection operators as there are group operators.

$$^{o}G = \sum_{\alpha}(X^{\alpha}_{C_1})^2 = \sum_{\alpha}(l^{\alpha})^2,$$

where $X^{\alpha}_{C_1}$ is the αth character of the class C_1. Thus, it is possible to invert Eq. (4.1) and expand group operators in terms of projection operators,

$$g = \sum_{\alpha}\sum_{i,j=1}^{l^{\alpha}} D^{\alpha}_{ij}(g)P^{\alpha}_{ij}. \tag{C3}$$

Normalization of the irreducible representation $|A^{\alpha}_{ij}\rangle$ is determined by Eqs. (C1), (C2), and (4.2),

$$\begin{aligned}\langle A^{\alpha}_{ij}|A^{\beta}_{kl}\rangle &= \langle A\,|P^{\alpha}_{ji}P^{\beta}_{kl}|A\rangle/(N^{\alpha}N^{\beta})^{1/2}\\ &= \{\langle A\,|P^{\alpha}_{jl}|A\rangle/N^{\alpha}\}\delta^{\alpha\beta}\delta_{ik}\\ &= \left(\frac{l^{\alpha}}{N^{\alpha}\,{}^{o}G}\right)\sum_{g\in G}D^{\alpha *}_{jl}(g)\langle A\,|gA\rangle\delta^{\alpha\beta}\delta_{ik}\\ &= \left(\frac{l^{\alpha}}{N^{\alpha}\,{}^{o}G}\right)\delta^{\alpha\beta}\delta_{ik}\delta_{jl} = \delta^{\alpha\beta}\delta_{ik}\delta_{jl}\\ &\therefore N^{\alpha} = \frac{l^{\alpha}}{{}^{o}G}.\end{aligned} \tag{C4}$$

Irreducible representation matrix elements of group operators, projection operators, and operators with the symmetry of the group are derived in Eqs. (C5), (C6), and (C7):

$$\begin{aligned}\langle A^{\alpha}_{ij}|g|A^{\beta}_{kl}\rangle &= \langle A\,|P^{\alpha}_{ji}gP^{\beta}_{kl}|A\rangle/(N^{\alpha}N^{\beta})^{1/2}\\ &= \sum_{\gamma}\sum_{m=1}^{l^{\gamma}}\sum_{n=1}^{l^{\gamma}} D^{\gamma}_{mn}(g)\langle A\,|P^{\alpha}_{ji}P^{\gamma}_{mn}P^{\beta}_{kl}|A\rangle/\\ &\quad (N^{\alpha}N^{\beta})^{1/2}\\ &= D^{\alpha}_{ik}(g)\{\langle A\,|P^{\alpha}_{jl}|A\rangle/N^{\alpha}\}\delta^{\alpha\beta}\\ &= D^{\alpha}_{ik}(g)\left(\frac{l^{\alpha}}{N^{\alpha}\,{}^{o}G}\right)\sum_{g'\in G}D^{\alpha *}_{ji}(g')\langle A\,|g'A\rangle\delta^{\alpha\beta}\\ &= D^{\alpha}_{ik}(g)\delta^{\alpha\beta}\delta_{jl},\end{aligned} \tag{C5}$$

$$\begin{aligned}\langle A^{\alpha}_{ij}|P^{\gamma}_{mn}|A^{\beta}_{kl}\rangle &= \langle A\,|P^{\alpha}_{ji}P^{\gamma}_{mn}P^{\beta}_{kl}|A\rangle/(N^{\alpha}N^{\beta})^{1/2}\\ &= \{\langle A\,|P^{\alpha}_{jl}|A\rangle/N^{\alpha}\}\delta^{\alpha\beta}\delta^{\alpha\gamma}\delta_{im}\delta_{nk}\\ &= \delta^{\alpha\beta}\delta^{\alpha\gamma}\delta_{im}\delta_{nk}\delta_{jl},\end{aligned} \tag{C6}$$

$$\langle A^{\alpha}_{ij}|\mathbf{K}|A^{\beta}_{kl}\rangle = \langle A|P^{\alpha}_{ji}\mathbf{K}P^{\beta}_{kl}|A\rangle/(N^{\alpha}N^{\beta})^{1/2}$$
$$= \{\langle A|\mathbf{K}P^{\alpha}_{jl}|A\rangle/N^{\alpha}\}\delta^{\alpha\beta}\delta_{ik}$$
$$\times(g\mathbf{K}=\mathbf{K}g;\ g\in G)$$
$$= \sum_{g\in G} D^{\alpha *}_{jl}(g)\langle A|\mathbf{K}|gA\rangle\delta^{\alpha\beta}\delta_{ik}\ . \qquad \text{(C7)}$$

[1]M. Hammermesh, *Group Theory and its Application to Physical Problems* (Addison Wesley, Reading, MA, 1972), p. 51.
[2]E. L. Muetterties, R. E. Merrifield, H. C. Miller, W. H. Knoth, and J. R. Downing, J. Am. Chem. Soc. **84**, 2506 (1962).
[3]L. A. Paquette, R. J. Ternansky, D. W. Balough, and G. Kentgen, J. Am. Chem. Soc. **105**, 5446 (1983).
[4]A. S. Pine, A. G. Maki, A. G. Robiette, B. J. Krohn, J. K. G. Watson, and Th. Urbanek, J. Am. Chem. Soc. **106**, 891 (1984).
[5]G. G. Christof, P. Engel, R. Usha, D. W. Balough, and L. A. Paquette, J. Am. Chem. Soc. **104**, 784 (1982).
[6]J. A. Wunderlich and W. N. Lipscomb, J. Am. Chem. Soc. **82**, 4427 (1960).
[7]J. M. Schulman and R. L. Disch, J. Am. Chem. Soc. **100**, 5677 (1978).
[8]R. L. Disch and J. M. Schulman, J. Am. Chem. Soc. **103**, 3297 (1981).
[9]D. A. Dixon, D. Deerfield, and G. W. Graham, Chem. Phys. Lett. **78**, 161 (1981).
[10]H. W. Kroto, J. R. Heath, S. C. O'Brien, R. F. Curl, and R. E. Smalley, Nature **318**, 162 (1985).
[11]T. Shibuya and M. Yoshitani, Chem. Phys. Lett. **137**, 13 (1987).
[12]Q. L. Zhang, S. C. O'Brien, J. R. Heath, Y. Liu, R. F.Curl, H. W. Kroto, and R. E. Smalley, J. Phys. Chem. **90**, 525 (1986); F. D. Weiss, J. L. Elkind, S. C. O'Brien, R. F. Curl, and R. E. Smalley, J. Am. Chem. Soc. **110**, 4464 (1988).
[13]W. G. Harter and D. E. Weeks, Chem. Phys. Lett. **132**, 387 (1986).
[14]W. G. Harter and D. E. Weeks, J. Chem. Phys. **90**, 4727 (1989).
[15]D. E. Weeks and W. G. Harter, Chem. Phys. Lett. **144**, 366 (1988).
[16]Z. C. Wu, D. A. Jelski, and T. F. George, Chem. Phys. Lett. **137**, 291 (1987).
[17]R. E. Stanton and M. D. Newton, J. Phys. Chem. **92**, 2141 (1988).
[18]M. Luo, G. Vriend, G. Kamer, I. Minor, E. Arnold, M. G. Rossmann, V. Boege, D. G. Scraba, G. M. Duke, and A. C. Palmenberg, Science **255**, 182 (1987).
[19]J. Hogle, M. Chow, and D. Filman, Sci. Am. **256**, 42 (1987).
[20]F. Doane and N. Anderson, *Electron Microscopy in Diagnostic Virology* (Cambrige University Press, Cambrdige, England, 1987), p. 51.
[21]D. J. Klein, T. G. Schmalz, G. E. Hite, and W. A. Seitz, J. Am. Chem. Soc. **108**, 1301 (1986).
[22]M. Hall, *The Theory of Groups* (Macmillan, New York, 1963), p. 1.
[23]B. L. Crawford and F. A. Miller, J. Chem. Phys. **17**, 249 (1949).
[24]D. Papousek and M. R. Aliev, *Molecular Vibrational–Rotational Spectra* (Elsevier, New York, 1982), p. 30.